# BONDED CONCRETE OVERLAY OF ASPHALT PAVEMENTS MECHANISTIC-EMPIRICAL DESIGN GUIDE (BCOA-ME): **ASSESSING THE NEED FOR PREOVERLAY REPAIRS WHEN CONSTRUCTION BCOA**

---

University of Pittsburgh
Department of Civil and Environmental Engineering
Pittsburgh, Pennsylvania 15261

*Prepared by:*

Tomas Adams
Julie M. Vandenbossche, Ph.D., P.E.

*Prepared for:*

FHWA Pooled Fund Project: TPF-5-165

August 2013

ABSTRACT

Design procedures developed for ultra-thin and thin whitetopping pavements identify the importance of the stiffness of the existing HMA pavement. Not yet considered is the effect that isolated areas of distressed HMA with reduced stiffness have on stress development in the thin whitetopping pavement. To determine the effect of isolated distressed areas, a FEM model is developed which considers longitudinal edge cracking to be the primary failure mode for thin whitetopping. A distressed area is introduced beneath the loading position which leads to this type of failure, and incrementally increased. The resulting change in critical stress is determined for the various structural characteristics that are likely encountered in the design of such pavements. Using regression analysis, an equation is developed that determines critical stress increase as a function of distressed area width and the stiffness ratio between non-distressed and distressed HMA. The stress increase factor found using this equation is applied to the critical stress determined for the non-distressed HMA. The increased critical stress can be used with existing design procedures to consider what effect the distressed area has on the design of ultra-thin and thin whitetopping pavement.

**TABLE OF CONTENTS**

## LIST OF TABLES

# LIST OF FIGURES

# 1 Introduction

Asphalt pavements account for 94 percent of the over 2 million miles of paved roads in the United States (National Asphalt Pavement Association, 2009). Of these roads, 19 percent are in poor to mediocre condition (U.S. Department of Transportation, 2011). With the addition of new lane miles to the U.S. roadway system at its lowest rate in decades, the focus has shifted from the design and construction of new pavements to the maintenance and rehabilitation of aging roads. A rehabilitation method that has recently gained popularity to extend the life of deteriorated asphalt pavements is the use of thin (TWT) and ultra-thin (UTW) whitetopping pavements; which refer to bonded concrete overlays of 2-4 in and 4-6 in respectively. This technique takes advantage of the less frequent maintenance and lower life cycle costs of Portland Cement Concrete (PCC), while utilizing the remaining structural capacity of the existing asphalt pavement to reduce design thicknesses.

A key consideration for the design of TWT and UTW pavements is the uniformity of the underlying HMA pavement (Darter, Hall, & Kuo, 1995). Areas that have reduced support conditions may require thicker overlays to be used (NCHRP, 2004). Unfortunately, a lack of understanding of how localized areas with reduced stiffness affect stress development in whitetopping overlays has made it difficult to effectively consider such areas in the design of UTW and TWT pavement. This study's objective is to quantify the effect of such areas for future consideration in the guidelines for the thin and ultrathin whitetopping pre-overlay repair.

## 1.1 Objective

The objective of this research is to contribute to the development of guidelines for identifying HMA sections in need of repair prior to the placement of a thin bonded concrete overlay. This contribution includes quantifying the effects that size and extent of distress in the existing HMA have on stress development in the bonded thin whitetopping overlay, thereby improving the performance of thin bonded concrete pavements, and facilitating the efficient expenditure of roadway rehabilitation funds.

## 1.2 Research Approach

The complex behavior of concrete bonded to distressed asphalt necessitates the use of the finite element method (FEM) to model stress development under traffic loadings. Influential model parameters are identified through a sensitivity analysis. A critical range of inputs for these parameters is then established by a review of typical design values. FEM runs are completed using combinations of these parameters to determine their effect on stress development in thin bonded concrete overlays.

# 2 Brief Overview of Whitetopping Pavements

Bonding concrete overlays to asphalt requires that they be more dependent on the integrity of the underlying pavement than would be necessary for an unbonded overlay. This is due to the composite behavior of the pavement structure. When fully bonded, the structural capacity of the existing HMA assists the PCC to reduce critical tensile stresses in the overlay. These stresses are a major design input in the thickness determination of whitetopping pavements. It follows then that properly characterizing the condition of the asphalt pavement is important to the design of well performing and cost effective thin bonded concrete overlays.

Visual inspection is currently used to identify areas requiring preoverlay repair. The extent and severity of distress is the deciding factor on whether or not to perform preoverlay repair; the subjective nature of this approach has led to a demand for more objective methods. Thus far, none of the currently available pavement evaluation methods, such as falling weight deflectometer (FWD) and laboratory testing, have been used to relate a localized area of reduced stiffness to the resulting increase in stress development of the UTW or TWT.

## 2.1 Considerations for the Design of Whitetopping Pavements

Whitetopping is a broad category of pavements that refers to the placement of a PCC overlay on an existing HMA pavement. Ultra-thin and thin whitetopping pavements are two specific subcategories within whitetopping that differ based on the thickness of the PCC overlay and bond assumption. Thin whitetoppings have PCC overlays 4 to 6 inches thick and will benefit from enhanced performance when bonded to the underlying HMA, but this bond is not necessary. Ultra-thin whitetoppings on the other hand, are 2 to 4 inches thick and require that they be bonded to the underlying HMA for satisfactory performance. Definitions for the categories of whitetopping are provided in Table 2.1.

**Table 2.1 Naming conventions based on whitetopping thickness.**

| Pavement Type: | PCC Overlay Thickness (in): | Bond Assumption |
|---|---|---|
| Conventional Whitetopping | > 6 | Unbonded |
| Thin Whitetopping | > 4 and ≤ 6 | Bonded or Unbonded |
| Ultra-thin Whitetopping | ≥ 2 and ≤ 4 | Bonded |

The benefits to both ultra-thin and thin whitetoppings from maintaining a bond between the PCC and HMA motivates special efforts to promote this bond such as texturing the surface of the existing HMA with a milling machine during construction of the whitetopping. Bonding the two pavements allows the pavement to perform as a composite structure, shifting the neutral axis downward, and thus reducing critical tensile stresses at the bottom of the PCC.

UTW and TWT pavements have similar design components as traditional PCC pavements. Environmental stresses are considered when designing the joint layout and the critical stress location for the expected mode of failure must be determined.

### 2.1.1 Environmental Stresses

Daily temperature fluctuations create gradients within the PCC overlay that must be considered during design. A positive temperature gradient develops when temperatures are higher at the top of the slab than at the bottom and the slab curls in a way that increases tensile stresses on the bottom of the PCC overlay. A negative temperature gradient develops when temperatures are higher at the bottom of the slab than at the top, and the slab curls in a way that increases tensile stresses on the top of the PCC overlay. Positive gradients are typically larger than negative gradients because of the effect solar radiation has on the rate of temperature increase at the surface of the PCC pavement.

Seasonally occurring uniform temperature changes also effect stress development in whitetopping pavements. Strains measured during the summer and in the winter with a similar temperature gradient show that higher average pavement temperatures resulted in greater measured strains (Vandenbossche, 2001). This result indicates that the reduction in HMA stiffness with an increase in HMA temperature influenced the structural support provided by the bonded HMA layer.

Moisture present beneath the surface affects whitetopping in much the same way as a negative temperature gradient. Increased moisture content at the bottom of the slab causes expansion of the pavement that will compound the effects of a negative temperature gradient and reduce the effects of positive temperature graident. Daily fluctuations will cause variation in the moisture content through the depth of the slab that can compound the effects of temperature gradients in the PCC slab (Vandenbossche, 2001).

To reduce the effect temperature has on the performance of bonded whitetopping pavements, the typical joint spacing range is reduced from the full-depth PCC standard of 12- to 20-ft intervals, to a more square spacing of 3- to 6-ft. By reducing the PCC panel size, a reduction in bending stresses due to the curling and warping caused by temperature and moisture gradients is realized.

### 2.1.2 Critical Stress Location

Previously developed UTW and TWT design procedures determine design stresses based on the assumed primary mode of failure. The two design procedures predominately used to design TWT and UTW are the American Portland Cement Association (ACPA) (Mack and Wu, 1997) and the Colorado Department of Transportation (CoDOT) (Sheehan et al., 2004) procedures, respectively. The APCA procedure developed for UTW, assumes corner breaks to be the primary failure mode, with the critical stresses occurring at the top of the PCC during corner loading in the presence of a negative gradient. The CoDOT procedure developed for TWT, assumes transverse cracking to be the primary failure mode, with critical stresses occurring at the bottom of the PCC during longitudinal edge loading at mid-slab in the presence of a positive gradient.

The APCA procedure used to design UTW, considers 2- to 4-in thick concrete overlays having panel sizes ranging from 2- x 2-ft to 4- x 4-ft. The CoDOT procedure is based on TWT overlays ranging between 4- to 7-in thick and having 4- x 4-ft, 6- x 6-ft, and 12- x 12-ft panel sizes. These, as well as the other parameters considered in development of both these procedures, are presented in Table 2.2.

**Table 2.2 Whitetopping structural parameters used in the development of the ACPA and CoDOT design procedures.**

| Parameters | ACPA | CoDOT |
|---|---|---|
| Panel size, ft | 2 x 2, 4 x 4 | 4 x 4, 6 x 6, 12 x 12 |
| $d_{PCC}$ , in | 2 - 4 | 4 - 7 |
| $E_{PCC}$, ksi | 4 | 4 |
| $d_{HMA}$ , in | 3 - 9 | 3, 6, 9 |
| $E_{HMA}$, ksi | 50 - 2,000 | 50, 250, 500, 750, 1,000 |
| k-value, psi/in | 75 - 800 | 50, 150, 300, 500 |

Performance evaluations of whitetopping test cells at MnROAD have found longitudinal cracks to occur more frequently in pavements with joint spacings greater than 4- x 4-ft; the design and performance of these test sections has been summarized in Table 2.3. Neither Cell 93 nor Cell 94, the only 4- x 4-ft panels for that test section, had any longitudinal cracks. These cells were also both UTW pavements; the only other UTW was Cell 95 which interestingly was one of the few cells with joint spacing greater than 4- x 4-ft to not have any longitudinal cracks.

The critical stress location influences the type of distress that propagates in the PCC and is one of the contributing factors to the differences in observed distresses for the MnROAD test section. When the critical stress occurs at the bottom of the PCC layer, cracks initiate along the edge of the PCC slab and will create longitudinal, transverse, or corner cracks depending on the meander of the crack. Critical stress at the top of the PCC layer will typically result in corner cracks.

**Table 2.3 Results from performance evaluation of MnROAD UTW and TWT test cells.**

| Cell | Age (yrs) | Traffic (Million ESALS) | $d_{PCC}$ (in) | $d_{HMA}$ (in) | Slab Size (ft x ft) | Corner Cracks | | Transverse Cracks | | Longitudinal Cracks | |
|---|---|---|---|---|---|---|---|---|---|---|---|
| | | | | | | Driving Lane | Passing Lane | Driving Lane | Passing Lane | Driving Lane | Passing Lane |
| 93 | 4 | 6.4 | 4 | 9 | 4 x 4 | 391 | 84 | 8 | 8 | 0 | 0 |
| 94 | 4 | 6.4 | 3 | 10 | 4 x 4 | 30 | 16 | 5 | 2 | 0 | 0 |
| 95 | 4 | 6.4 | 3 | 10 | 5 x 6 | 43 | 6 | 9 | 4 | 0 | 0 |
| 92 | 11.5 | 9.8 | 6 | 7 | 10 x 12 | 0 | 0 | 0 | 0 | 3 | 6 |
| 96 | 11.5 | 9.8 | 6 | 7 | 5 x 6 | 0 | 0 | 0 | 0 | 1 | 0 |
| 97 | 11.5 | 9.8 | 6 | 7 | 10 x 12 | 0 | 0 | 0 | 0 | 7 | 0 |
| 60 | 4.5 | 3.8 | 5 | 7 | 5 x 6 | 0 | 0 | 0 | 0 | 3 | 0 |
| 61 | 4.5 | 3.8 | 5 | 7 | 5 x 6 | 0 | 0 | 2 | 0 | 5 | 4 |
| 62 | 4.5 | 3.8 | 4 | 8 | 5 x 6 | 0 | 0 | 0 | 22 | 0 | 0 |
| 63 | 4.5 | 3.8 | 4 | 8 | 5 x 6 | 7 | 1 | 3 | 0 | 8 | 5 |

**$d_{PCC}$: PCC layer thickness**
**$d_{HMA}$: HMA layer thickness**

Another factor in influencing the distress propagation is the wheelpath. A consequence of the reduced panel size for UTW and TWT pavements is that the location of the longitudinal joints will coincide with the wheelpath. This has been reported as resulting in corner breaks for UTW sections where the wheelpath is located along a longitudinal joint (Vandenbossche & Fagerness, 2002). Panels smaller or equal to 4- x 4-ft have the wheelpath landing close to the longitudinal joint, Figure 2.1, while larger panel sizes have the wheelpath closer to mid-panel, Figure 2.2. The location of the wheelpath influences where the cracks initiate and the type of distresses that manifest.

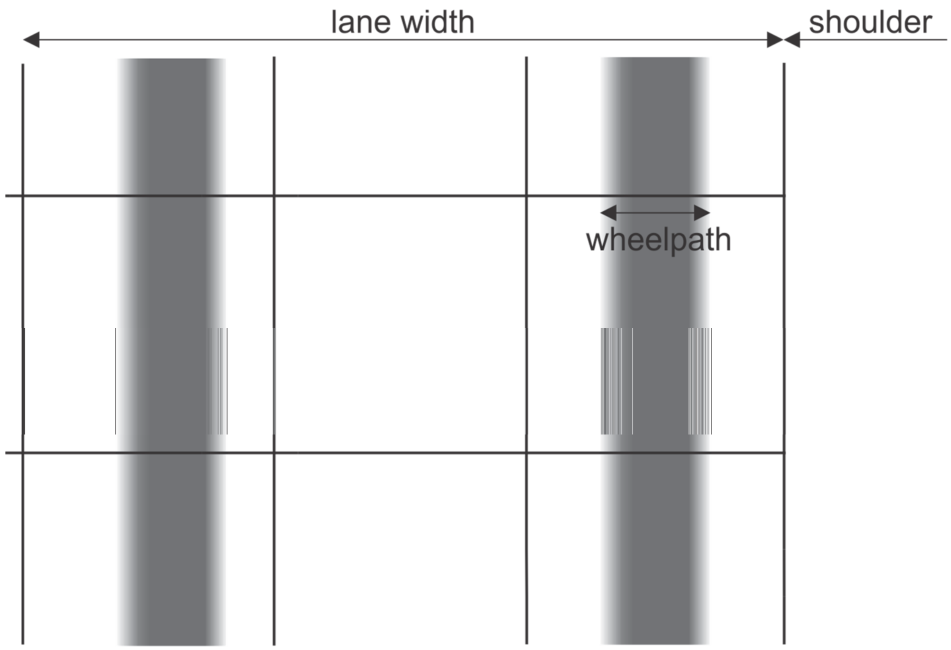


**Figure 2.1 Wheelpath in 4- x 4-ft thin whitetopping sections.**

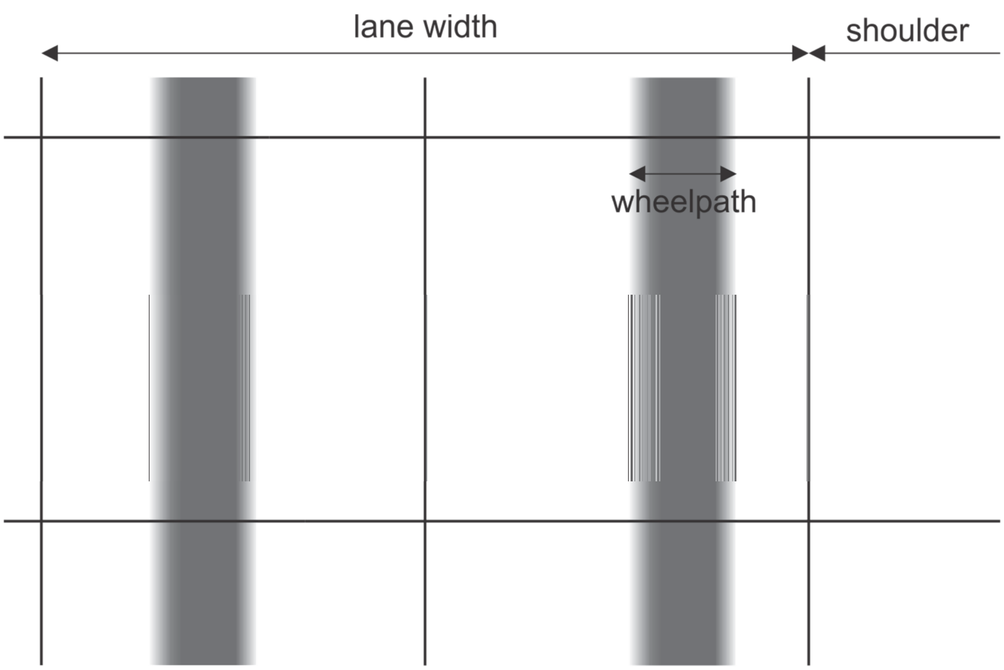


**Figure 2.2 Wheelpath in 6- x 6-ft thin whitetopping sections.**

## 2.2 PCC Fatigue Consumption

The useful life of a PCC pavement is a function of its condition. After a certain level of deterioration, the condition of the pavement is such that it is no longer suitable to carry traffic. In PCC pavements, this deterioration can lead to cracking. One way then to establish the design life of a PCC pavement is to attribute pavement failure to a certain percentage of slabs that have cracked (American Concrete Paving Association (ACPA), 1998).

Since pavements rarely crack after a single load repetition, material fatigue is considered to incorporate the effect of cyclic loading on the slab. Utilizing forecasted traffic loadings, along with equations that predict the critical stress generated for a given load, the number of load repetitions to failure can be estimated (Mack & Chung Lung Wu, 1997)

A key assumption for PCC pavements is that below a certain magnitude of stress, no damage is accumulated in the pavement, and it would theoretically have an infinite lifetime. Design of such a pavement for all load levels would not be practical. The concepts of reliability were introduced into the fatigue consumption equation so that pavements could be designed to reach the functional life requirement with a degree of statistical certainty necessary to the roadway classification (Riley, Titus-Glover, Mallela, Waalkes, & Darter, 2005).

$$log(N_{PCC}) = \left[-\frac{SR^{-10.24}log(R)}{0.0112}\right]^{0.217} \qquad \textit{Equation 2.1}$$

$N_{pcc}$: *number of load repetitions to failure*

$SR$: *stress ratio ($\sigma_{max}/MOR$)*

$R$: *desired level of reliability*

By better understanding the stress development in a particular pavement structure, the functional lifetime of the pavement can be better predicted. This allows improved management of the rehabilitation spending for an agency. The results of this study will provide such an improvement by determining the stress increase caused by a distressed area beneath a whitetopping pavement.

## 2.3 Effect of Distress in Existing HMA

The underlying HMA layer has a significant effect on the behavior of the bonded concrete overlay. Distress in the HMA creates a non-uniform support system that has deleterious effects on the performance of UTW and TWT. The following is a discussion of the distress that can be present in the existing HMA, as well as the influences of these distresses on the performance of the overlay.

### 2.3.1 Rutting

Repeated loadings in the wheelpath of an HMA pavement can lead to permanent deformations in the pavement known as rutting. Rutting in the existing HMA pavement is a problem for UTW and TWT if it indicates a weak subgrade or a pavement whose binder type makes it susceptible to permanent deformation. Mild rutting not related to these conditions can be ignored for the preparation of a PCC overlay (Smith, 1993) and may even prove beneficial, providing increased PCC thickness in the wheelpath where stresses are the highest (NCHRP, 2004). When the rutting is severe but not related to underlying support deficiencies, it is typically treated successfully through milling of the HMA layer prior to placement of the overlying PCC. Through these procedures, the effect of rutting on the performance of UTW and TWT pavements is minimized.

### 2.3.2 Fatigue Cracking and Thermal Cracking

Excessive strain in the HMA pavement under wheel loads leads to fatigue cracking. Fatigue cracking in the existing HMA will produce a non-uniform support condition for the PCC overlay or, if severe, interfere with bond development between the HMA and PCC. Large, transverse cracks, such as those caused by thermal contraction of the pavement, have also been found to reflect into thinner bonded PCC layers when the HMA is significantly stiff relative to the overlay, Figure 2.3 (Vandenbossche & Barman, 2010). For minor cracking, the non-uniformity created by the reduction in HMA stiffness is not generally felt to be significant (National Concrete Pavement Technology Center, 2008).

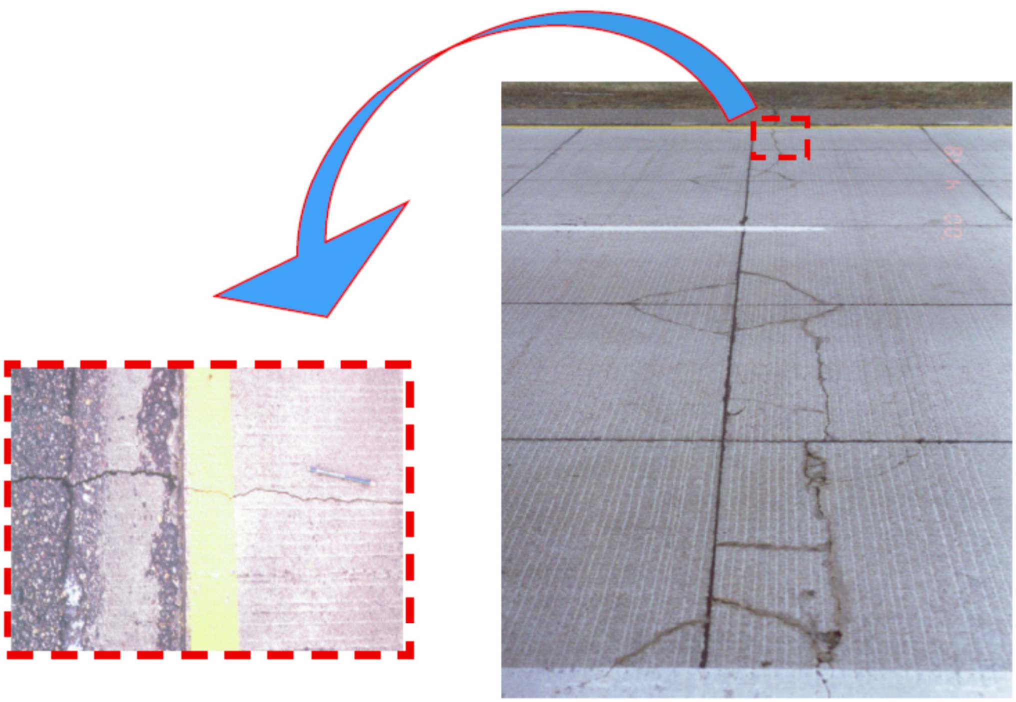

**Figure 2.3 Reflective cracking in thin bonded concrete overlay. (Vandenbossche & Barman, 2010)**

### 2.3.3 Raveling

HMA pavements with a binder susceptible to moisture degradation will unravel when exposed to moisture for prolonged periods, leaving the unbound aggregate, a condition known as stripping. Stripping in the existing HMA indicates a severe moisture problem that will reduce the level of support in affected areas, leading to an increase in the non-uniformity. It also significantly effects bond development between the HMA and PCC by reducing the composite behavior of the resulting monolithic structure and thereby decreasing performance of the bonded PCC overlay. Since the cause of this distress is often moisture present below the surface, the severity and extent of this problem is typically worse at the bottom of HMA pavements.

## 2.4 Treatment of HMA distress prior to PCC overlay

Most distresses in the existing HMA are not directly treated prior to bonded whitetopping placement due to the high costs involved or from a lack of justification for the repair provided by available design guides. A commonly performed pre-overlay procedure known as milling, removes many surface distresses, such as rutting, by removing the top 2-3 inches of age hardened asphalt. Where distresses cannot simply be removed by milling of the HMA surface, conventional methods of HMA pavement repair can be performed prior to placement of the overlay.

Simply replacing distressed HMA with fresh HMA is a repair technique known as patching. Patching has been used to prevent moisture from entering through the distressed area and further deteriorating support conditions by weakening the underlying layers. This rehabilitation method does not address the subgrade failures that cause many distresses and for this reason, can only be considered a temporary remedy. Caution must be used with this method in preparation for bonded overlays as it has been reported that the PCC overlay does not bond well to the freshly placed HMA (National Concrete Pavement Technology Center, 2008).

To address HMA distress related to underlying layers, full depth repairs (FDR) are used to remove the entire pavement structure, possibly including any underlying support layers, and replacing it with a similar structure or one redesigned to address any support issues. To avoid the poor bond fresh HMA creates and simplify preoverlay rehabilitation, it may be more cost effective to fill the area removed during full depth repairs with fresh concrete while placing the whitetopping overlay.

Large cracks in the existing HMA cause different distresses in the PCC overlay depending on the condition of the cracks. Deteriorated cracks are likely related to a subgrade failure and may require FDR to prevent failure of the PCC overlay. Non-deteriorated cracks, such as those due to thermal expansion, may reflect cleanly into the PCC overlay if preventive measures are not taken. Measures such as applying tar paper to act as a bond breaker between the PCC and cracked HMA have been reported to effectively reduce the incidence of crack reflection (Vandenbossche & Fagerness, 2002). Although not a common practice, saw cutting the PCC joints directly over the cracked HMA is an option that can reduce stress concentrations caused by movement of the HMA.

## 2.5 Preoverlay Evaluation Methods

To account for the effect of the existing HMA on thin bonded concrete overlays first involves evaluating its condition as accurately as possible. According to a survey conducted by the

National Cooperative Highway Research Program (NCHRP), 90% of respondents use some sort of visual inspection to evaluate the condition of the existing HMA, 45% use falling weight deflectometer (FWD) data, and 7% use laboratory testing (NCHRP, 2004). Ideally, all three would be used. Unfortunately, budget restrictions typically prevent the opportunity to do all three. Therefore, the designer must understand the strengths and weaknesses of each tool and formulate an evaluation plan that balances these considerations with budgetary constraints.

A distress survey involves mapping the location and severity of distresses in the pavement through visual inspection. In order to meaningfully categorize some distresses, it is necessary to understand the cause of the distress. Further investigations into the cause of the distress are conducted based on the type of distress being evaluated. Steps taken can include collecting core samples of the different pavement layers, gathering FWD data, or conducting laboratory tests of in-situ material samples.

The FWD is used to evaluate the pavement by applying a load simulating that caused by a wheel load onto the pavement and measuring the resulting surface deflections, Figure 2.4. The measured deflection basin can be used to describe the stiffness of the different pavement structural layers. FWD testing is used extensively by agencies for project characterization, as it can help identify localized areas of reduced support and quantify overall project uniformity. Advances in the application of FWD testing have made it possible to gather information over miles of roadway relatively inexpensively, as compared to other destructive evaluation methods.

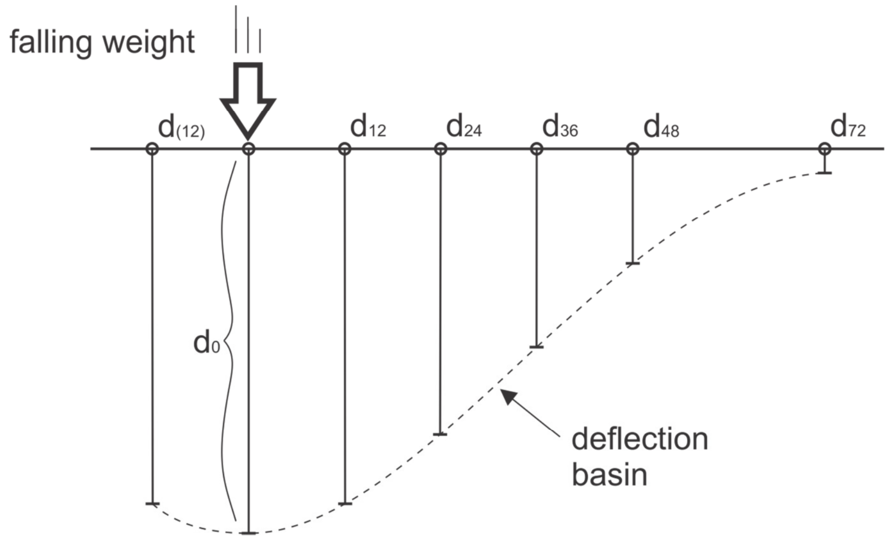


**Figure 2.4 Falling Weight Deflectometer (FWD) deflection basin.**

FWD data has also been used to estimate useful pavement design parameters, such as elastic modulus, by using what is referred to as backcalculation. This technique iteratively solves for the layer's elastic modulus by using elastic layer theory.

The data collected from FWD testing is of limited use on its own and is best utilized in conjunction with other evaluation methods. If a distress survey is available, a designer may compare areas where the FWD tests indicate a reduction in support to see if it can be attributed to a distress. If there was no surface distress, then further testing may be necessary to determine the cause. Unfortunately, the effect of localized areas with reduced HMA stiffness is not well understood, and little guidance is available on its effect on the performance of thin bonded concrete overlays. Deciding what level of reduced stiffness is necessary to address, and what can be ignored, is subjectively based on the experience of the designer and may not effectively correlate to the actual performance of the overlay.

Although not routinely performed due to high costs, laboratory testing of samples taken from the in-situ pavement can provide information on the material properties of the HMA that can then be related to pavement performance. However, since bonded concrete overlays are a relatively newer pavement rehabilitation option, the complex behavior of the composite material is not as well defined mechanistically as more traditional pavement structures. This limits the usefulness of the information that can be determined from laboratory testing, making cost justification even more difficult.

Using FEM modeling techniques, the effect that a localized distressed HMA region has on stress development in whitetopping pavements can be considered in the preoverlay evaluation. This study will develop a model that represents a critical loading scenario in whitetopping pavements over a localized area of deteriorated HMA. The resulting stress increase attributable to the HMA condition can then be used to modify the design stresses in commonly used design procedures. This information will help agencies to better evaluate the appropriateness of preoverlay repairs when using thin whitetopping pavements as a rehabilitation technique.

# 3 Model Description

Determining the effect of distressed HMA on stress development within a thin bonded concrete overlay in this study is accomplished through the use of the Finite Element Method (FEM). FEM is especially well suited for modeling TWT, due to the limitations of closed form solutions in accounting for the composite behavior of PCC bonded to HMA. Since FEM is such a computationally intensive technique, the finite element analysis suite ABAQUS was used. A section of whitetopping pavement was modeled in ABAQUS, and the critical stresses generated under an applied load were estimated. Significant structural parameters were identified and then varied to investigate their interaction with the distressed HMA.

### 3.1 Modeling Pavement Layers

A six slab model with 6-ft joint spacing, as shown in Figure 3.1, was used to represent a section of TWT adjacent to an unbound shoulder. Twenty seven node brick elements were utilized for modeling both the PCC and HMA layers. The loaded PCC panel had 2,592 total elements of equal size, 36 x 36 x 2 (W x L x H). The other 5 PCC panels each had 324 elements of equal size, 18 x 18 x 1.

Load transfer between adjacent PCC panels was accomplished through spring elements that act in the direction of loading. Each PCC joint face had approximately 108 springs mimicking the contribution of aggregate interlock. Spring stiffness was varied in the model until reasonable LTE values were produced, (80 to 90%). No interaction was modeled for the exterior faces of the PCC panels since the displacements 72" away from loading were not sufficiently large to enact aggregate interlock at these joints.

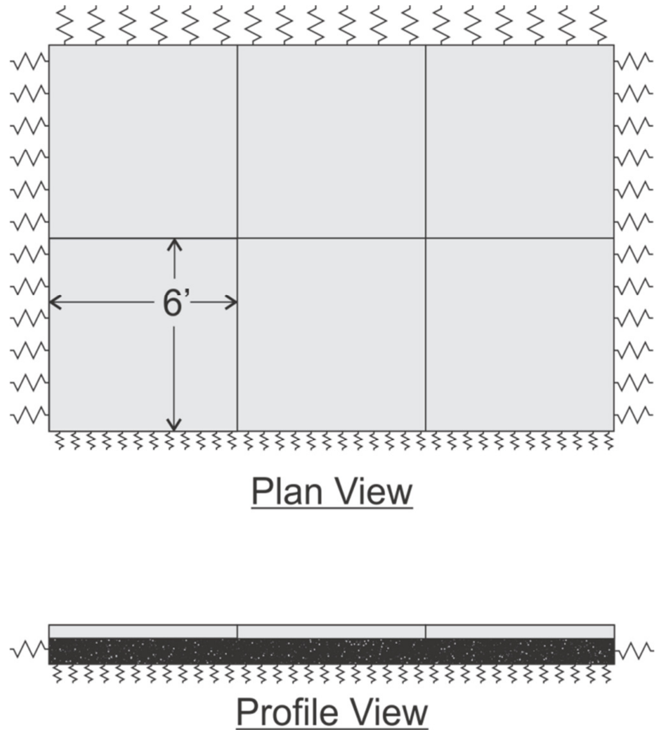


**Figure 3.1 Model Layout.**

Beneath the PCC panels was a continuous HMA solid with 1,944 total elements of equal size, 54 x 36 x 1.

The continuous HMA was tied to the PCC at every node on the face between the two materials, in order to simulate a completely bonded interface between the two materials. An exception to this was a 4 inch boarder adjacent to the loaded PCC panel. The small un-tied boundary was introduced to eliminate stress singularities caused by nodes from two separate PCC panels being tied to the same node on the HMA surface, see Figure 3.2.

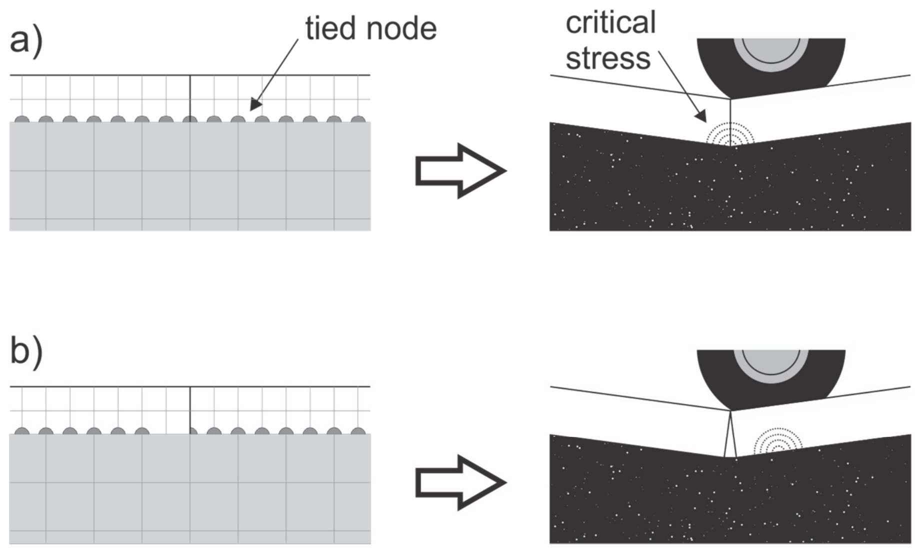


**Figure 3.2 a) Stress singularity created when two nodes in the PCC layer are tied to a single node on the HMA layer. b) Critical stress when nodes along the loaded slab joint in the adjacent slab are not tied.**

A Winkler spring foundation was used to model the composite stiffness of all layers below the HMA layer. A spring constant, k, was assigned to the spring foundation based on a range of typical design values.

### 3.2 Model Boundary Conditions

A Winkler spring foundation was used to simulate continuation of the pavement at the boundary of the model, see Figure 3.1. A uni-directional elastic linear assumption was used for the HMA that approximated the elastic modulus of this material as a spring with equivalent stiffness acting in the normal direction. This assumption approximated the results of a larger HMA layer but had reduced computational time. For the model boundaries at the shoulder, a spring constant was chosen to simulate an unbound granular material that responds like the subgrade.

## 3.3 Model Constants

Certain material properties, such as density and Poisson's ratio, are needed for the simulation but do not significantly affect stress development. Poisson's ratios of 0.35 and 0.18 are used for the HMA and PCC, respectively. The density of both materials was set at 140 pcf. The elastic modulus of the PCC was set at 4,500 ksi.

## 3.4 Model Loading

Loading was applied in the wheelpath along the transverse edge. The critical stress for this loading location occurs at the bottom of the PCC layer directly beneath loading for most pavement structures. There are scenarios where the critical stress can occur at the top, such as during corner loading with a loss of support beneath the PCC slab. In this situation, the slab acts as a cantilever to create critical stresses at the top of the slab some distance away from loading. Typically though, bending stresses directly beneath the load create the critical tensile stresses in the PCC slab. For this reason, the critical stress location for this study is considered as being at the bottom of the PCC layer, directly beneath the loading.

As discussed in a previous section, failure in pavements can be considered in terms of a summation of fatigue damage of the PCC material. Since this damage is incurred over many repetitions, only the area of the pavement that is subjected to the majority of the loading repetitions, the wheelpath, is considered in this study. The load in the wheelpath was adjacent to a transverse joint.

The shape of the loading area selected for this study, as shown in Figure 3.3, is an approximation of a dual tire foot print based on typical tire sizes and spacing as described by the

Mechanistic Empirical Design Guide (MEPDG) (ARA, Inc. ERES Consultants Division, 2004). The width of a truck tire from sidewall to sidewall is given as roughly 12 inches, with the spacing between the centerlines of tires as also roughly 12 inches. The footprint of the load area is based on the measurements taken at MnROAD by Mike Helfert in 1996. These show that the effective contact area width is narrower than the gross tire width.

A single square tire loading area was commonly used in the development of previous whitetopping design procedures. Preliminary runs were made as part of this study and it was determined that the critical stress generated in the PCC overlay was sensitive to the loading area, as shown in Table 3.1. The pavement properties used to generate Table 3.1 were selected to represent typical conditions. A dual tire was used for this study, as it better approximates real-world loading condition of critical truck loads.

**Table 3.1 Loading area shape sensitivity**

| Loading Area | dual | single |
|---|---|---|
| Critical Stress | 121 psi | 149 psi |
| Change in Loading Area, Δ% | 23% | |
| HMA Thickness, $D_{HMA}$ | 6 in | |
| HMA Stiffness, $E_{HMA}$ | 640 ksi | |
| HMA Poisson's Ratio, $\mu_{HMA}$ | 0.35 | |
| PCC Thickness, $D_{PCC}$ | 4 in | |
| PCC Stiffness, $E_{PCC}$ | 4,500 ksi | |
| PCC Poisson's Ratio, $\mu_{PCC}$ | 0.18 | |
| Pressure | 93.75 psi | |

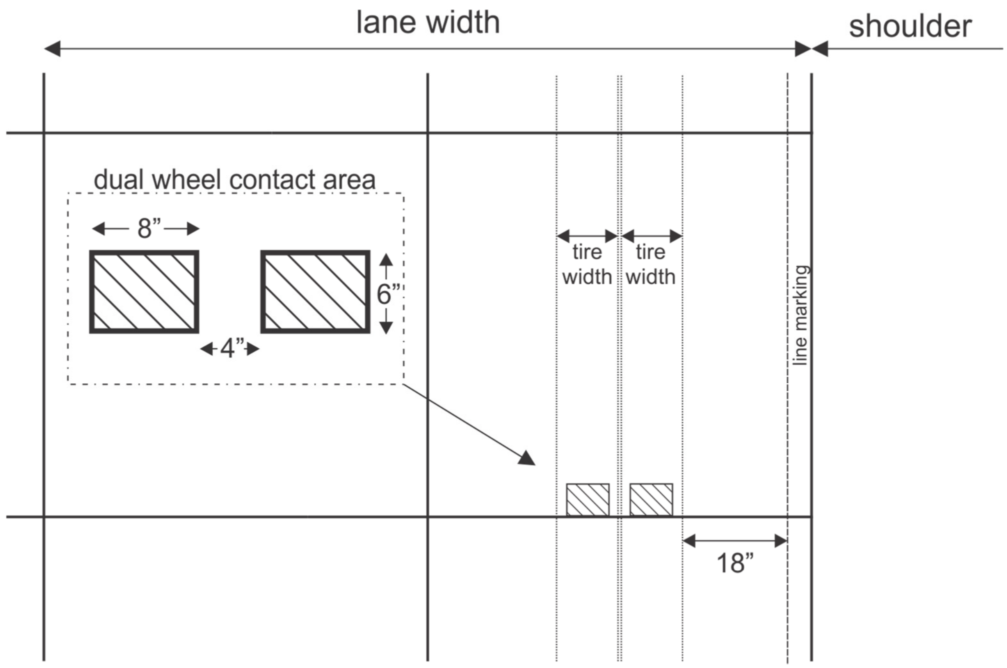


**Figure 3.3 Loading area detail**

The dual tire was placed in the default wheelpath given by the MEPDG as 18 inches from the edge of pavement markings to the edge of the wheel. To model the effect of distressed HMA on bonded PCC overlays, it is assumed that the distress is creating an area of reduced stiffness in the HMA. This distressed area is assigned a reduced elastic modulus with respect to the undamaged HMA sections. The shape of this distressed area, as shown in Figure 3.4, is controlled in the longitudinal direction but has an infinite width in the transverse direction. Although there are many more possible shapes of the distressed area, it is necessary to limit the number of variations in this study for the sake of feasibility. Since distressed areas are often larger at the bottom of the pavement than the top, the width of the distressed area will increase 8 inches at each 3 inch depth interval, as shown in Figure 3.5.

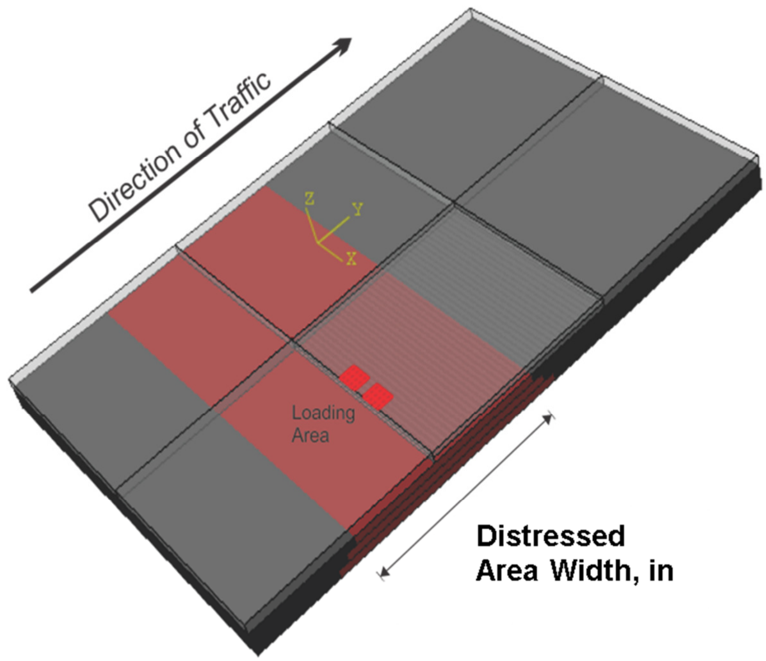


**Figure 3.4 Shape of distressed area.**

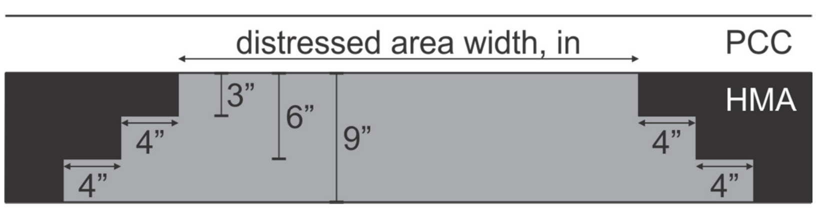


**Figure 3.5 Slab profile showing an increase in distressed area with depth.**

Orientation of the distressed HMA beneath the load was selected based on that which produced the greatest critical stresses. A pavement with the properties described in Table 3.2 has a distressed HMA area of a constant size placed in three different positions in relation to the loading. These orientations are as follows: justified adjacent to the joint, centered beneath loading, and justified to the edge of loading away from the joint, Figure 3.6. The results from these runs show that critical stresses are highest when loading occurs centered in the distressed area. See Table 3.3.

**Table 3.2 Description of pavement structure used to investigate effect of distressed area size and orientation.**

| | |
|---|---|
| HMA Thickness, $D_{HMA}$ | 3 in |
| Undamaged $E_{HMA}$ | 1,280 ksi |
| Damaged $E_{HMA}$ | 320 ksi |
| $\mu_{HMA}$ | 0.35 |
| PCC Thickness, $D_{PCC}$ | 4 in |
| PCC Stiffness, $E_{PCC}$ | 4,500 ksi |
| PCC Poisson's Ratio, $\mu_{PCC}$ | 0.18 |
| Pressure | 93.75 psi |

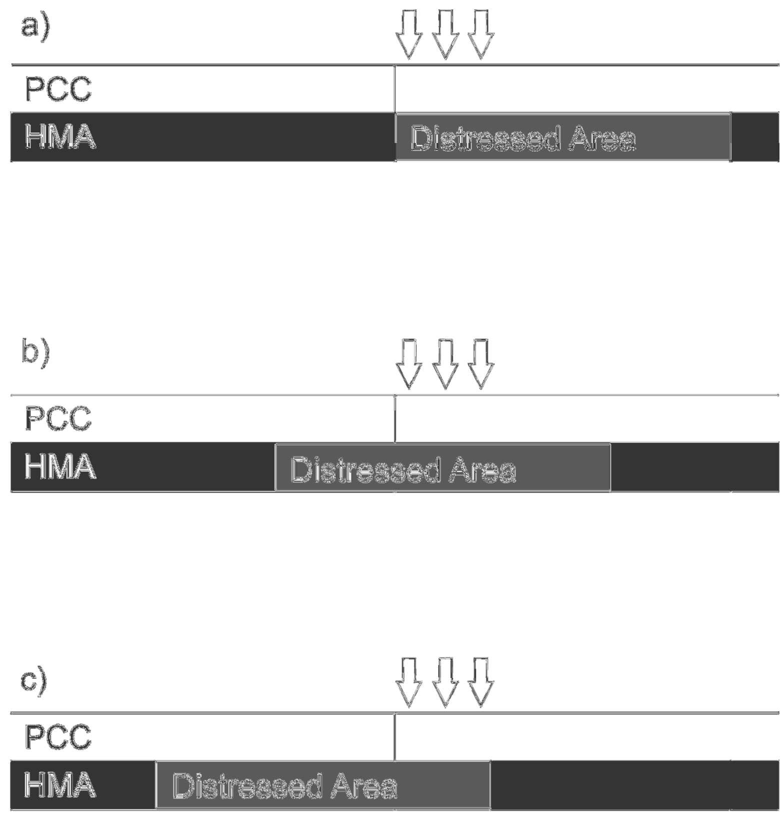


**Figure 3.6 a) Distressed area justified adjacent to joint. b) Distressed area centered beneath loading. c) Distressed area justified to the edge of loading away from joint.**

**Table 3.3 Critical stress with the HMA distress area oriented as shown in Figure 3.6.**

| Distress Orientation | Critical Stress, psi |
|---|---|
| Figure 3.4 a) | 298 |
| Figure 3.4 b) | 309 |
| Figure 3.4 c) | 287 |

The minimum distressed area width was selected to minimize the effect that the abrupt transition from distressed to non-distressed HMA has on stress development. To determine what minimum distress width to use, a pavement with the properties described in Table 3.2 was modeled with a distressed area centered beneath the load. This area grew from a width that places the boundary at the edge of the load, to a width of 72-in.

Plotting the critical stress as a function of the change in distressed area width revealed unusually high critical stresses at relatively narrow distressed areas, see Figure 3.7. The results at 8- and 16-in distressed area widths did not follow the expected trend between distressed area width and magnitude of critical stress, which was for the stresses to increase as the size of distress increases. This unexpected increase is attributed to the limitations of modeling using finite elements where an abrupt boundary exists between elements with substantially different material properties. Since this stress increase is not representative of a real world condition, only distressed area widths 16-in and greater were used to limit this effect.

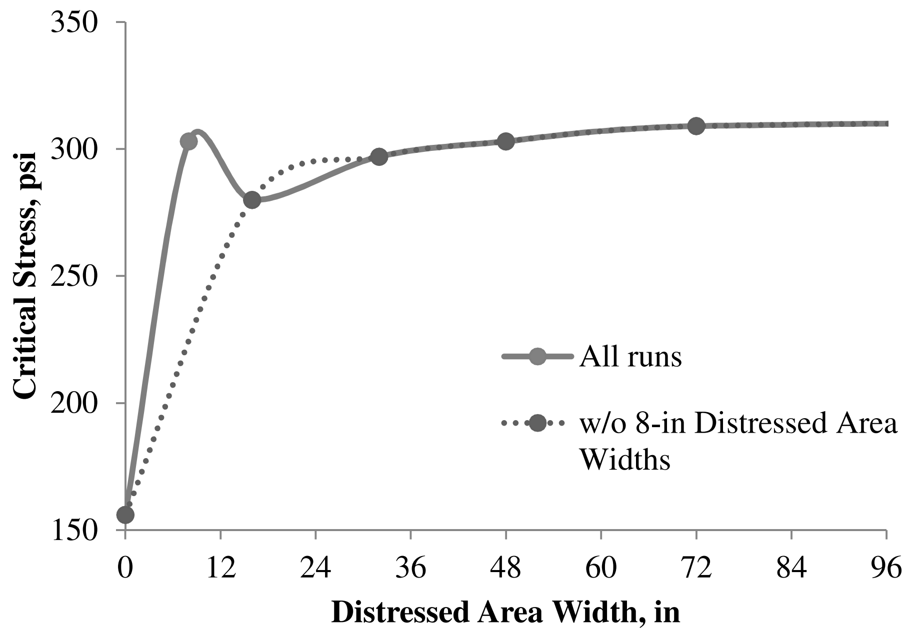


**Figure 3.7 Critical stress as a function of distressed area width for a pavement with structural properties as given in Table 3.2.**

## 3.5 Model Validation

Validation of the FEM model was accomplished by comparing calculated deflections with measured deflections for whitetopping sections at the Minnesota Road Research Facility (MnROAD). For this comparison, structural parameters representing those measured for the MnROAD whitetopping sections were used in the FEM model. These parameters are summarized in Table 3.4. The resulting deflection basins for both the MnROAD test section and the FEM model are shown in Figure 3.8. As can be seen, good agreement was found between the two deflection basins.

**Table 3.4 Structural properties from MnROAD whitetopping Cell 62 used for model validation.**

| | |
|---|---|
| HMA Thickness, $D_{HMA}$ | 8 in |
| HMA Stiffness, $E_{HMA}$ | 350 ksi |
| HMA Poisson's Ratio, $\mu_{HMA}$ | 0.35 |
| PCC Thickness, $D_{PCC}$ | 4 in |
| PCC Stiffness, $E_{PCC}$ | 4,900 ksi |
| PCC Poisson's Ratio, $\mu_{PCC}$ | 0.13 |
| Load Level | 9,140 lbs |
| Time | 1:05 PM |
| Surface Temperature | 114.4 °F |

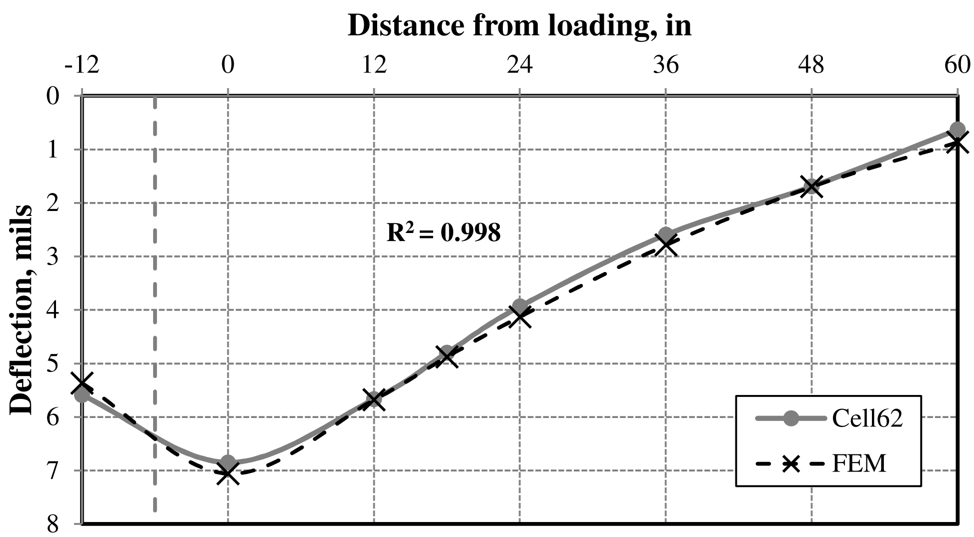


**Figure 3.8 Deflection basins from MnROAD Test Cell 62 and FEM model with similar structural parameters.**

# 4 Experimental Design

## 4.1 Parameter selection

Structural characteristics influential to the response of thin bonded concrete overlays are determined. The only parameters chosen are those that affect the stress response of the thin bonded concrete overlay and that are reasonably likely to vary for different pavement structures. From this investigation, the following parameters are selected:

- *HMA thickness,* $D_{HMA}$
- *Non-distressed HMA elastic modulus,* $E_{HMA(undmg)}$
- *Distressed HMA elastic modulus,* $E_{HMA(dmg)}$
- *PCC thickness,* $D_{PCC}$
- *Distress size*

Notably absent is PCC joint load transfer, a measure of how well load is transferred across pavement joints. This finding is reasonable, as load has been found to be primarily transferred across the joint through the HMA layer in ultra-thin whitetopping (Mack & Chung Lung Wu, 1997). Further evidence of this is provided in the next section.

### 4.1.1 Whitetopping Sensitivity to PCC Aggregate Interlock

For simple slab-on-grade concrete pavements, the degree of load transferred across a joint through the contact between exposed aggregate on the joint faces and the underlying support layers, significantly reduces stresses in the PCC when loaded near the joint. Between 70-80% of load is transferred through the aggregate interlock in the PCC layer with the rest being transferred through the base. When a stabilized base layer is used, a higher proportion of the load is transferred through the layers below the slab, 30-40%. The aggregate interlock is still the dominant mechanism by which load is transferred, but this increase in the load transferred through the subsurface pavement layers by an improvement to the structural capacity of the layers demonstrates the important role that these layers can play in joint performance.

In whitetopping pavements, the presence of the HMA layer below the surface PCC layer further increases the proportion of load transferred through the pavement layers below the PCC layer. To what extent that this load transfers through the HMA base layer has not been well understood. Further complicating this interaction is the temperature sensitivity of both the HMA stiffness and aggregate interlock.

As the HMA layer temperature increases, the stiffness of the layer decreases. If the majority of load is being transferred through this layer in whitetopping pavements, then the LTE would be expected to decrease as temperatures rise. Offsetting this effect would be that at higher temperatures, the space between the PCC layer joints decreases, creating a stiffer joint and thereby increasing LTE. To investigate what extent these mechanisms affect load transfer, FWD test results from MnROAD ultra-thin and thin whitetopping test sections are reviewed.

The ultra-thin whitetopping sections were designated Cell 93, 94, and 95. Of these, Cell 93 was a 4 inch PCC layer bonded to a 9 inch HMA layer. Both Cells 94 and 95 were 3 inch PCC layers bonded to 10 inch HMA layers. Cells 93 and 94 had 4- x 4-ft joint spacing and Cell 95 had 6W- x 5L-ft joint spacing. Cell 95 also contained fibers in the PCC layer.

The thin whitetopping sections were designated Cell 96 and 97. Both cells were 6 inch PCC layers over a 7 inch HMA layer. The only difference between the two designs is that Cell 96 had 6W- x 5L-ft joint spacing and Cell 97 had 12W- x 10L-ft joint spacing.

FWD tests were performed in the wheelpath at two joints within each test section numerous times over a 4 year period (1998-2001). In addition to FWD testing, these sections were instrumented with thermocouples that allowed the HMA layer mid-depth and PCC surface temperature to be recorded at the time of testing.

Using this information, plots of LTE versus HMA mid-depth temperature were created, as shown in Figure 4.1 through Figure 4.5.

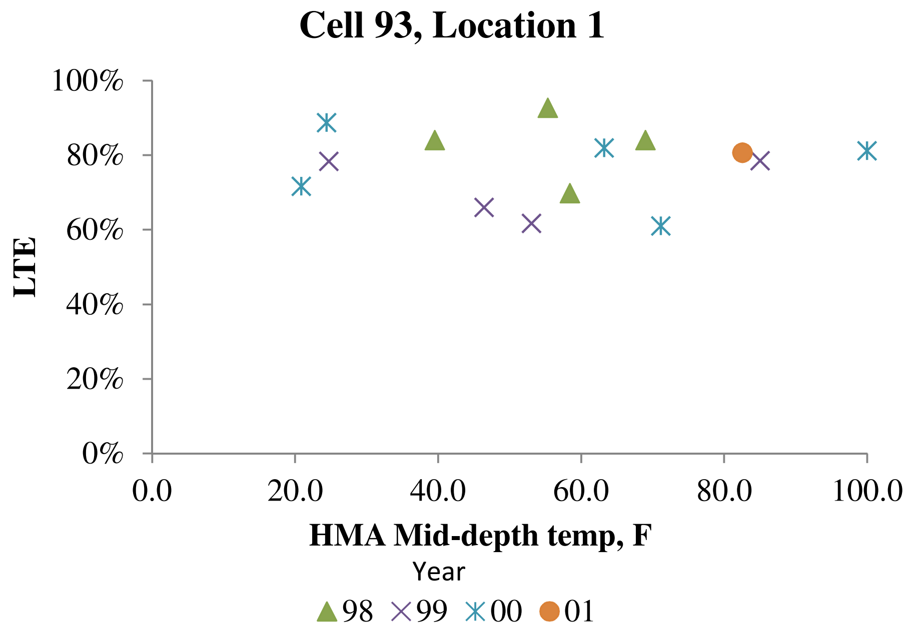


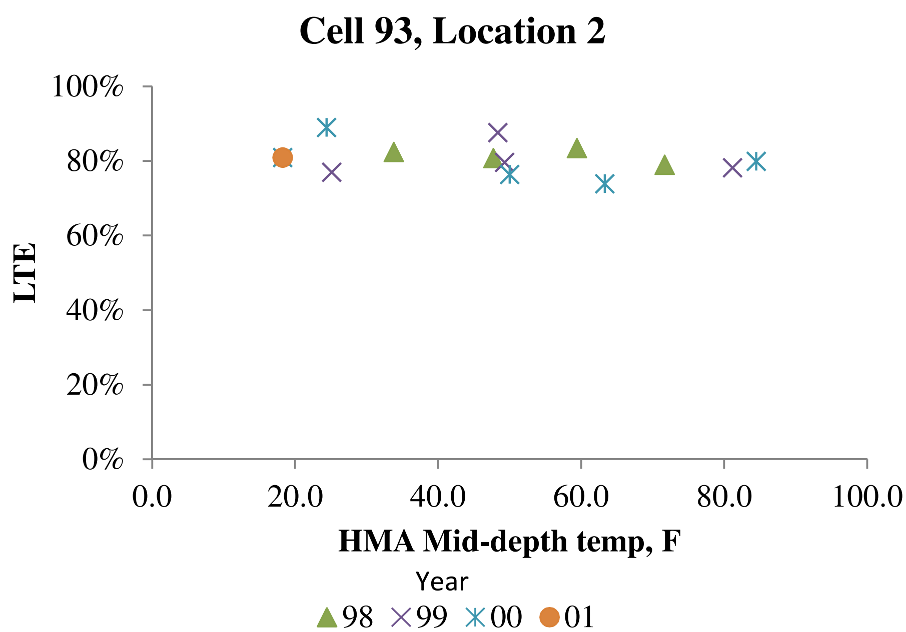


**Figure 4.1 LTE vs. HMA Mid-depth temperature for Cell 93 Locations 1 and 2 from MnROAD.**

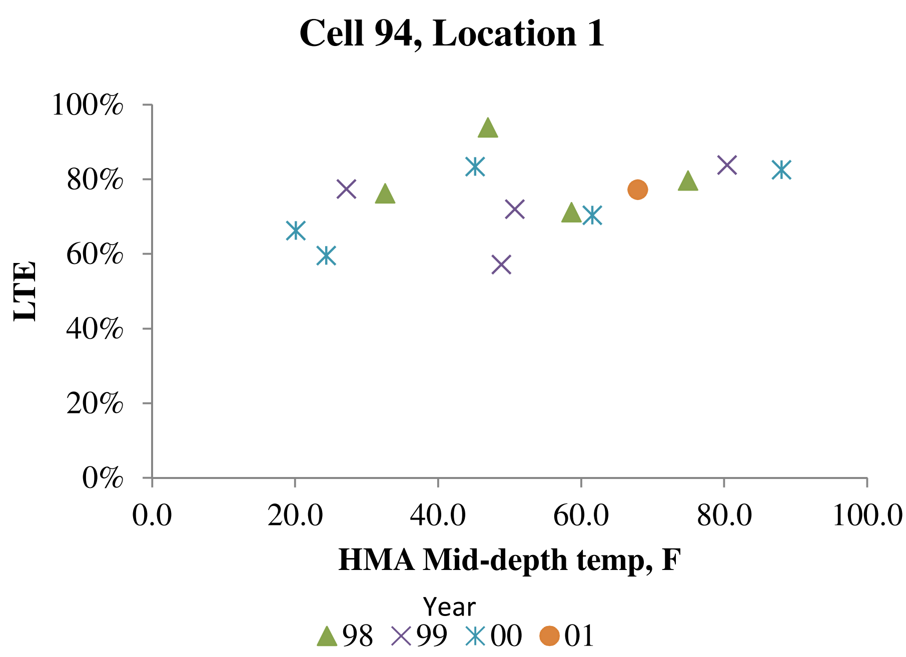


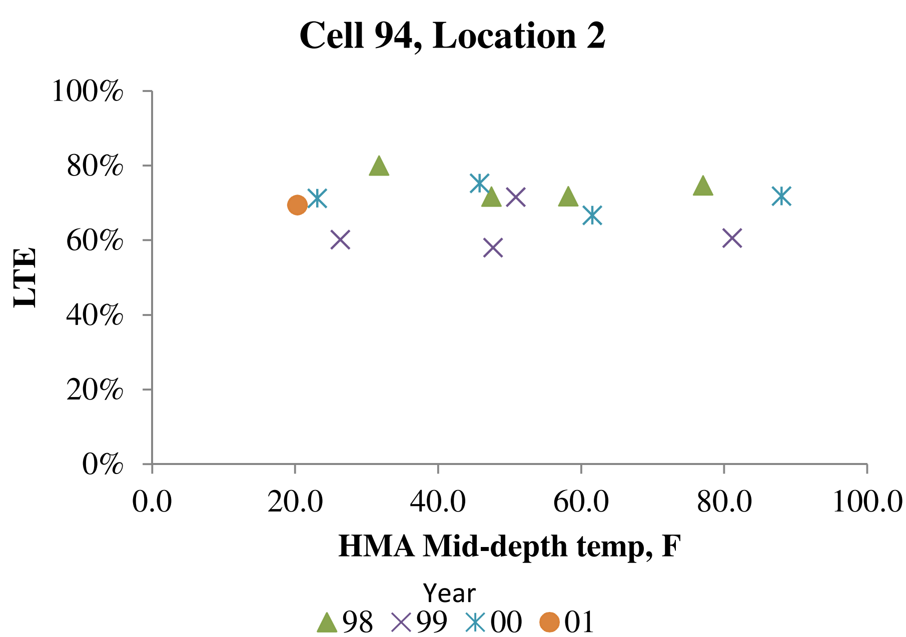


**Figure 4.2 LTE vs. HMA Mid-depth temperature for Cell 94 Locations 1 and 2 from MnROAD.**

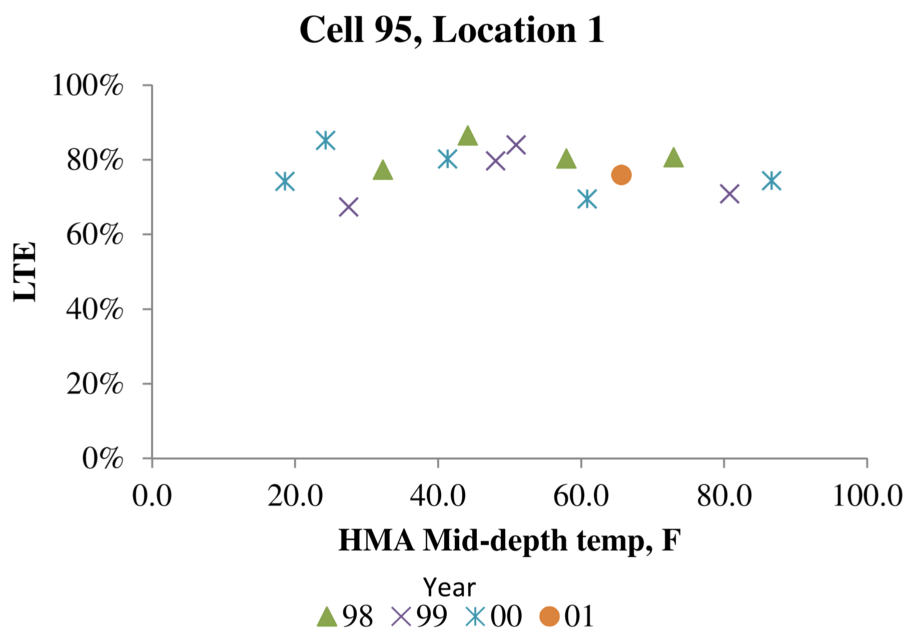


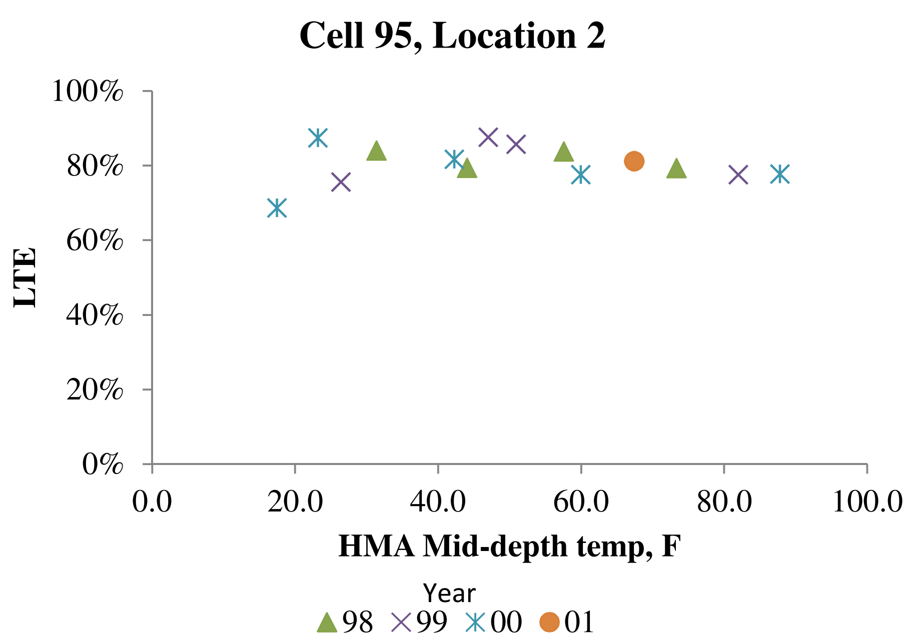


**Figure 4.3 LTE vs. HMA Mid-depth temperature for Cell 95 Locations 1 and 2 from MnROAD.**

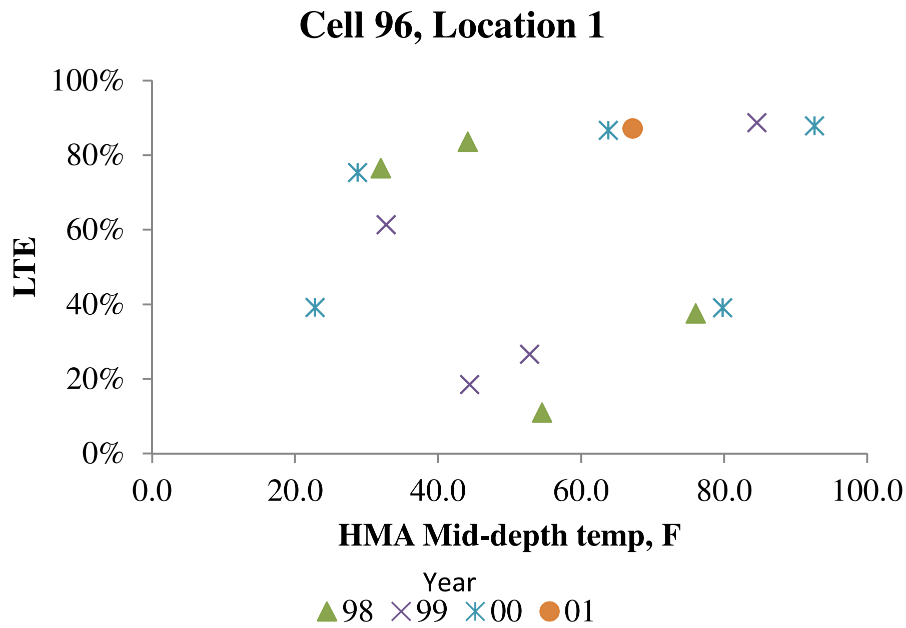


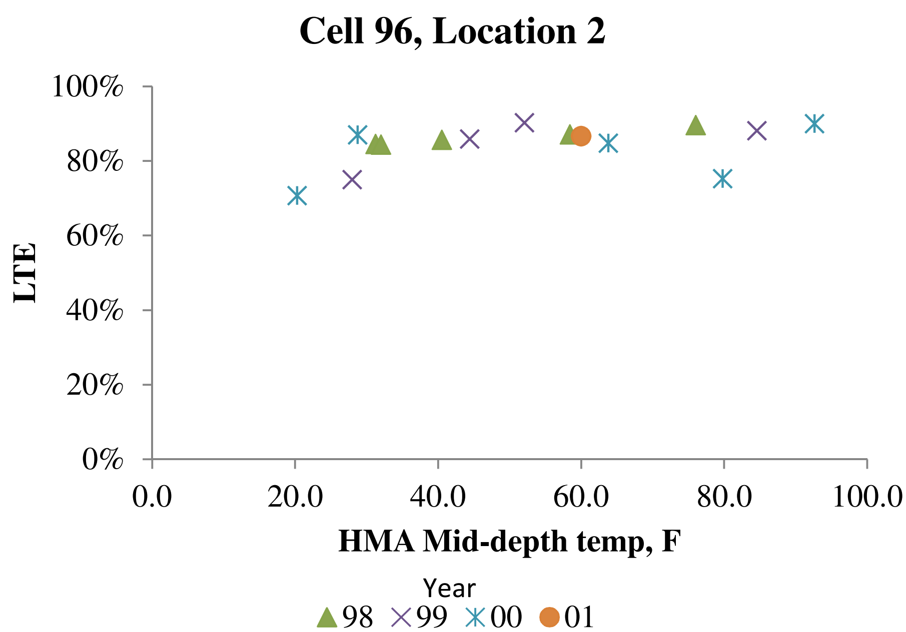


**Figure 4.4 LTE vs. HMA Mid-depth temperature for Cell 96 Locations 1 and 2 from MnROAD.**

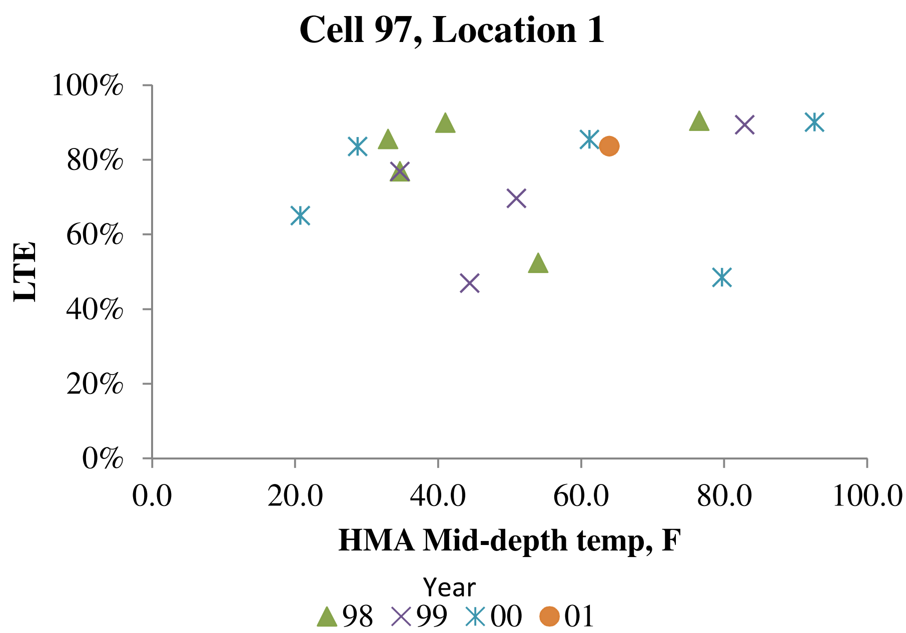


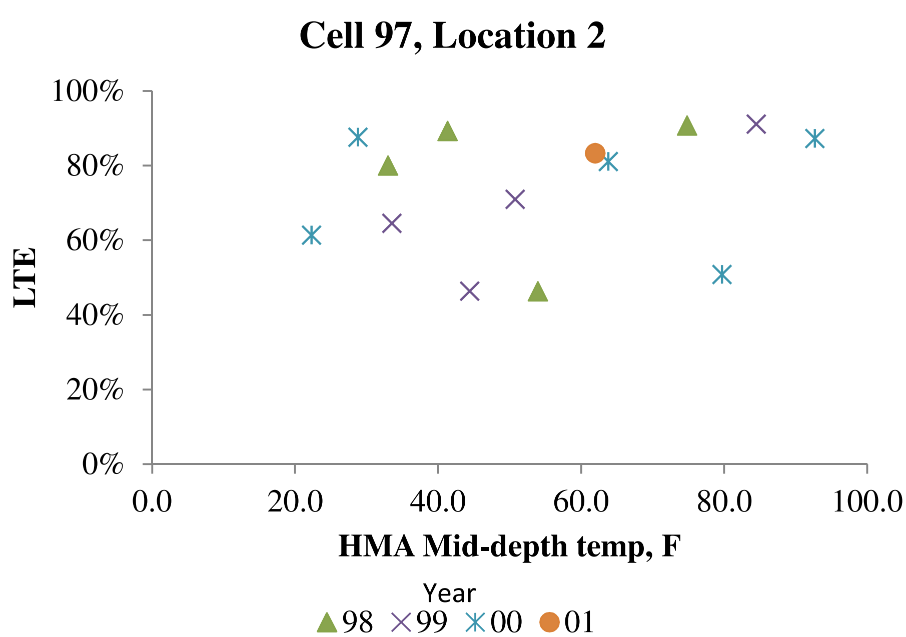


**Figure 4.5 LTE vs. HMA Mid-depth temperature for Cell 97 Locations 1 and 2 from MnROAD.**

From these plots it is apparent that a variety of mechanisms are at work. For the ultra-thin whitetopping sections (Cells 93-95), some joints have a greater variation in LTE than other joints, even within the same cell. The coefficients of variation (COV) were calculated for each of these cells to allow a comparison of the relative magnitudes of this variation, Table 4.1.

**Table 4.1 Coefficient of Variation (COV) of LTE for MnROAD ultra-thin whitetopping test sections.**

| | COV |
|---|---|
| Cell 93 Joint 1 | 0.12 |
| Cell 93 Joint 2 | 0.05 |
| Cell 94 Joint 1 | 0.13 |
| Cell 94 Joint 2 | 0.09 |
| Cell 95 Joint 1 | 0.08 |
| Cell 95 Joint 2 | 0.06 |

An explanation for the differences in magnitude of variation even within the same Cell requires that the structural condition of the joint be considered. Joints are formed by cutting a specified depth into the pavement at the desired locations. The depth of this cut does not descend through the entire pavement layer; rather it weakens the pavement sufficiently to lead to eventual crack development under normal environmental and traffic loadings. In some instances, the crack will only form within every other sawed joint due, to the stress relief provided by adjacent cracks.

The difference in magnitude of variation between FWD test locations within a cell, for instance Cell 93, indicates that one of the joints being tested may have failed to have the crack propagate the entire depth of the PCC layer. In such a situation, the continuity of the PCC layer at the joint would primarily control LTE, limiting variation attributable to the other LTE influencing factors that have been discussed.

Cell 94 also displays a difference in the magnitude of variation between test locations although the absolute magnitude of the variation is higher than that seen in Cell 93 for both locations. This indicates that both joints have likely cracked, and the difference in variation is due to the complex interaction of the other LTE influencing factors.

Interestingly Cell 95 has a reduced magnitude of variation for both test locations. It should be highlighted that this cell contained structural fibers that are meant to improve the performance of cracks developed in the PCC layer by resisting separation and opening of the crack. These results indicate that that the fibers are contributing to the increased continuity of the PCC layer at the joint.

Another potentially influential factor to LTE that has not yet been discussed is a scenario where the crack at the joint propagates not only through the PCC layer, but through the entire HMA layer as well. This becomes more likely to occur as the relative stiffness of the PCC layer increases with respect to the HMA layer (Vandenbossche & Fagerness, 2002). For the MnROAD test sections, Cell 96 and 97 have the highest relative stiffness of the PCC layer with respect to the HMA layer, 6-in PCC over 7-in HMA, and are thus most likely to have the HMA layer cracked at the PCC joints.

Evidence that the crack at the joint has propagated down through the HMA layer is provided by low LTE measurements observed for some of the joints in Cell 96 and 97. At low ambient temperatures, minimal engagement of aggregate interlock is occurring between the crack surfaces in the two paving materials and the load is primarily being transferred through the base layers. In this scenario, LTE measurements would approach those described earlier as being transferred through a bound or unbound base material, 20-40%.

Three of the four FWD test location in Cell 96 and 97 had LTE measurements lower than 50% indicating that load is primarily being transferred through the support layers beneath the HMA. Further evidence supporting this claim is provided by comparing LTE to subgrade temperature throughout the year. Using the temperature data from 2000, the bottom most sensor 14 inches below the surface for Cell 97, the LTE measured at different times of year is compared with the corresponding subgrade temperatures, Figure 4.6.

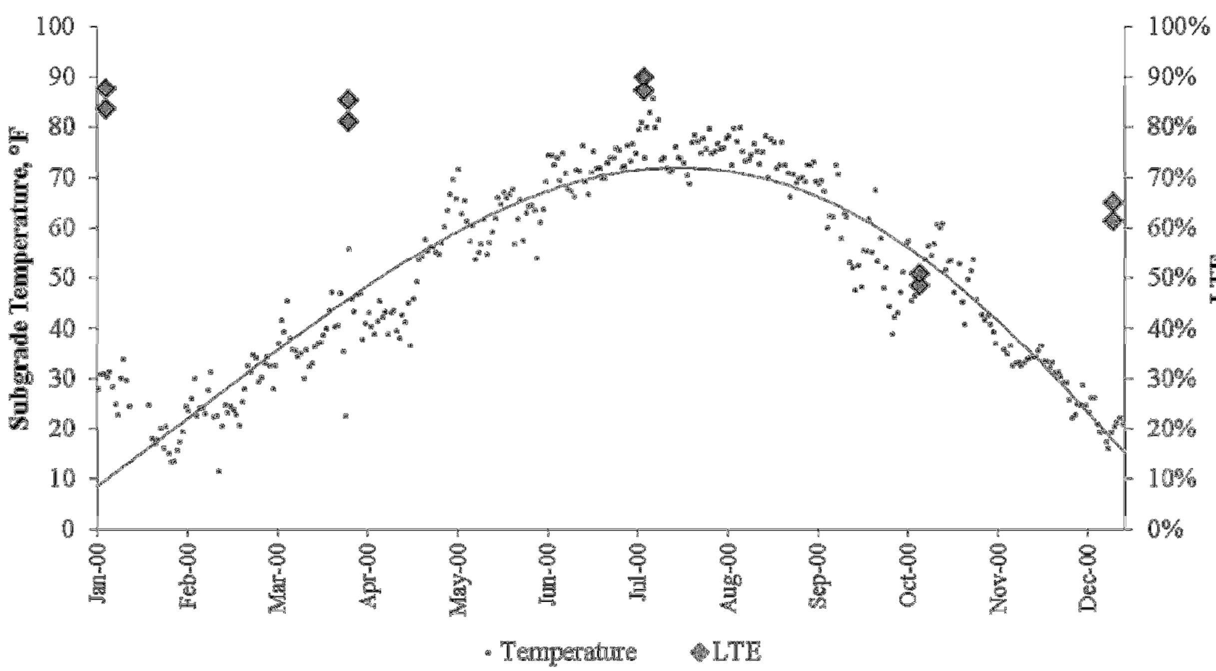


**Figure 4.6 Subgrade Temperature and LTE from 1/1/2000 to 12/31/2000 in Cell 97 at MnROAD.**

The LTE was found to be the lowest during the fall when the subgrade would be saturated but not frozen. A few months later, the continually dropping temperatures indicate that the subgrade is now frozen and the LTE clearly rebounds. In the spring, there is some delay between the temperature reading at the bottom sensor that was 14 inches below surface, and the thawing of the entire subgrade whose frost line  was measured at 55 inches below the surface according to historical frost thaw depth measurements taken that year in nearby Ostego, MN. This explains why high LTE values are still found in the end of March as the temperature at 14 inches below the surface begins to rise above freezing.

From this analysis of FWD data for the whitetopping test sections at MnROAD, it has been shown that a discontinuity in a paving layer such as a joint, introduces a complex interaction between temperature sensitive materials that leads to increased variation in the LTE. Further, when this discontinuity is present in multiple paving layers, the magnitude of possible variation increases even more.  By comparing situations where only the PCC layer is cracked, with situations when the transverse crack propagates through the HMA layer, an estimate for the percent of load being transferred through the intact HMA layer is found to be 60-70%.  This rate was determined using the MnROAD test sections where the minimum HMA thickness was 7 inches.  HMA layers thinner than 7 inches may contribute less to the LTE.

For this analysis where no crack is present in the HMA model, it is assumed that varying the degree of aggregate interlock is insignificant, as it will only provide marginal improvements. The spring stiffness is therefore set at a constant value that provides an approximate LTE of 90%.

## 4.2 Establish Inputs

After identifying what parameters significantly influence stress development in UTW and TWT pavements, the range of values considered for each input was established.  The number of values selected for each parameter must be balanced between the expected significance of the response non-linearity and computational time. Depending on the interaction of the parameter with the pavement structure, a range of values or a single critical value was selected.

The elastic modulus of the asphalt layer, for instance, has a significant effect on stress development over a wide range of values. It was necessary then to use a larger range values in the analysis to account for this. As the stress development was expected to be non-linear, values were chosen following a base-2 exponential increase.

The parameters included in this study are provided in Table 4.2.

**Table 4.2 Parameters included in the analysis.**

| | |
|---|---|
| $D_{HMA}$, in | 3, 6, 9 |
| Undamaged $E_{HMA}$, ksi | 320, 640, 1280 |
| Damaged $E_{HMA}$, ksi | 80, 160, 320, 640 |
| $D_{PCC}$, in | 4, 6 |
| Distressed Area width, in | 16, 32, 48, 72, ALL |

*ALL indicates that the HMA stiffness is equal to that of the Damaged $E_{HMA}$ throughout the pavement.

### 4.2.1 Assumptions

A limited number of preliminary FEM runs were completed to determine if any assumptions could be made about the interaction between the model parameters and the stress response. These trends would allow for a reduction in the total number of runs, and thus reduced computation time.

The first assumption was that the transition from non-distressed to distressed HMA was modeled artificially abrupt. This caused an overly conservative stress response for scenarios where loading takes place near the distress boundary. Figure 4.7 presents the FEM results that include scenarios where the loading area is near the distress boundary (less than 6 inches). As can be seen in Figure 4.7, the extent of this increase is a function of the magnitude of difference in stiffness between the non-distressed and distressed HMA. The minimum distressed area width used for this study was 16" to prevent the distress boundary from significantly increasing the stress response.

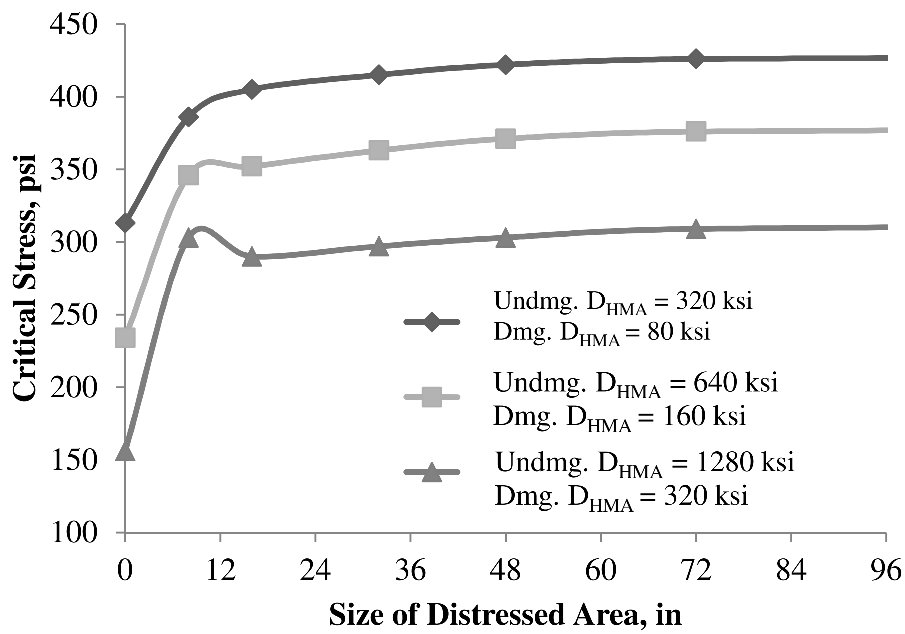


**Figure 4.7 Critical stress increase as a function of distressed area size including a distressed area equal to 8-in when $D_{HMA}$ = 3 in and $D_{PCC}$ = 4 in.**

The next assumption was that stress development, as a function of distressed area size, is dependent on the ratio of non-distressed HMA stiffness ($HMA_s$) to distressed HMA stiffness ($HMA_w$). Simplifying this expression reduced it to a ratio of the elastic modulus for the non-distressed and distressed HMA. This ratio will be referred to hereafter as the Elastic Modulus Ratio (EMR), as shown in Equation 4.1.

$$EMR = \frac{HMA_s}{HMA_w} \qquad \textit{Equation 4.1}$$

*$HMA_s$: Elastic modulus of non-distressed HMA, psi*

*$HMA_w$: Elastic modulus of distressed HMA, psi*

At a certain distress size, further increasing the size of the distressed area does not significantly affect the magnitude of critical stresses in the overlay. This stress will be referred to hereafter as the maximum critical stress (MCS). The MCS wasdetermined by calculating critical stress in the overlay using an elastic modulus value for the entire HMA layer that is equivalent to that approximated for just the distressed area. Assuming the rate that stress in the overlay approaches MCS, as being dependent on EMR, allowed for it to be quickly approximated.

The final assumption was that the interaction between the PCC thickness and the thickness of the distressed HMA is not significant. Or in other words, the behavior of the thin bonded overlay stress response to variation in MR and distress size is independent of the PCC thickness. That is not to say that different PCC thicknesses result in the same critical stress for a given HMA pavement structure. Only that the change in critical stress caused by the presence of distressed HMA is similar for pavements with different PCC thicknesses.

A single PCC thickness, 4 inches, was used when determining the effect of EMR and distress size on critical stress development. The effect of the distress variables was extrapolated for a 6 inch PCC thickness. This is done by adding the increase in critical stress caused by the distress variables to the non-distressed HMA critical stress response at the alternate PCC thickness.

### 4.2.2 FEM Runs

To quantify the effect of distressed HMA underlying thin bonded concrete overlays, 90 runs were completed using the finite element analysis software suite ABAQUS.

Of these runs, 30 were completed using an HMA layer with a homogenous elastic modulus. This is to establish a baseline for comparison with the results of runs featuring a distressed area in the HMA layer. The structural parameters used for these runs were as follows:

- HMA elastic modulus, ksi: 80, 160, 320, 640, 1280
- HMA thickness, in: 3, 6, 9
- PCC thickness, in: 4, 6

The effect of different size areas of distressed HMA was investigated using 60 runs. The structural parameters used for these runs are as follows:

- Non-distressed HMA elastic modulus, ksi: 320, 640, 1280
- Distressed HMA elastic modulus, ksi: 80, 160, 320
- Distressed area size, in: 16, 32, 48, 72
- EMR: 2, 4, 8
- HMA thickness, in: 3, 6, 9
- PCC thickness, in: 4

# 5 Results and Discussion

## 5.1 Stress Response of FEM Model with Non-distressed HMA.

The stress response of the model containing only non-distressed HMA is presented in Table 5.1. These results were used as a baseline for comparison with the stress response of the model containing distressed HMA.

**Table 5.1 Stress response of modeled whitetopping with non-distressed HMA.**

| $D_{HMA}$, in | $E_{HMA}$, ksi | $D_{PCC}$, in | $\sigma_{critical}$ |
|---|---|---|---|
| 3 | 80 | 4 | 428 |
| 3 | 160 | 4 | 379 |
| 3 | 320 | 4 | 313 |
| 3 | 640 | 4 | 234 |
| 3 | 1280 | 4 | 156 |
| 6 | 80 | 4 | 346 |
| 6 | 160 | 4 | 273 |
| 6 | 320 | 4 | 196 |
| 6 | 640 | 4 | 121 |
| 6 | 1280 | 4 | 57 |
| 9 | 80 | 4 | 294 |
| 9 | 160 | 4 | 222 |
| 9 | 320 | 4 | 149 |
| 9 | 640 | 4 | 87 |
| 9 | 1280 | 4 | 37 |
| 3 | 80 | 6 | 260 |
| 3 | 160 | 6 | 236 |
| 3 | 320 | 6 | 201 |
| 3 | 640 | 6 | 158 |
| 3 | 1280 | 6 | 112 |
| 6 | 80 | 6 | 224 |
| 6 | 160 | 6 | 183 |
| 6 | 320 | 6 | 140 |
| 6 | 640 | 6 | 95 |
| 6 | 1280 | 6 | 54 |

| $D_{HMA}$, in | $E_{HMA}$, ksi | $D_{PCC}$, in | $\sigma_{critical}$ |
|---|---|---|---|
| 9 | 80 | 6 | 200 |
| 9 | 160 | 6 | 156 |
| 9 | 320 | 6 | 111 |
| 9 | 640 | 6 | 71 |
| 9 | 1280 | 6 | 37 |

## 5.2 Stress Response of FEM Model with Distressed HMA.

The stress response of the model containing distressed HMA is presented in Table 5.2. These results were used to determine the effect of distress in the HMA layer on the critical stress in the PCC overlay.

**Table 5.2 Stress response of modeled whitetopping with distressed HMA.**

| $D_{HMA}$, in | $E_{HMA(undmg)}$, ksi | $E_{HMA(dmg)}$, ksi | $D_{PCC}$, in | Distressed Area Width, in | $\sigma_{critical}$ |
|---|---|---|---|---|---|
| 3 | 320 | 80 | 4 | 0 | 313 |
| 3 | 320 | 80 | 4 | 16 | 405 |
| 3 | 320 | 80 | 4 | 32 | 415 |
| 3 | 320 | 80 | 4 | 48 | 422 |
| 3 | 320 | 80 | 4 | 72 | 426 |
| 3 | 320 | 80 | 4 | ALL | 428 |
| 6 | 320 | 80 | 4 | 0 | 196 |
| 6 | 320 | 80 | 4 | 16 | 316 |
| 6 | 320 | 80 | 4 | 32 | 330 |
| 6 | 320 | 80 | 4 | 48 | 338 |
| 6 | 320 | 80 | 4 | 72 | 344 |
| 6 | 320 | 80 | 4 | ALL | 346 |
| 9 | 320 | 80 | 4 | 0 | 149 |
| 9 | 320 | 80 | 4 | 16 | 270 |
| 9 | 320 | 80 | 4 | 32 | 281 |
| 9 | 320 | 80 | 4 | 48 | 287 |
| 9 | 320 | 80 | 4 | 72 | 292 |

**Table 5.3 Stress response of modeled whitetopping with distressed HMA. (cont.)**

| $D_{HMA}$, in | $E_{HMA(undmg)}$, ksi | $E_{HMA(dmg)}$, ksi | $D_{PCC}$, in | Distressed Area Width, in | $\sigma_{critical}$ |
|---|---|---|---|---|---|
| 9 | 320 | 80 | 4 | ALL | 294 |
| 3 | 640 | 160 | 4 | 0 | 234 |
| 3 | 640 | 160 | 4 | 16 | 352 |
| 3 | 640 | 160 | 4 | 32 | 363 |
| 3 | 640 | 160 | 4 | 48 | 371 |
| 3 | 640 | 160 | 4 | 72 | 376 |
| 3 | 640 | 160 | 4 | ALL | 379 |
| 6 | 640 | 160 | 4 | 0 | 121 |
| 6 | 640 | 160 | 4 | 16 | 250 |
| 6 | 640 | 160 | 4 | 32 | 260 |
| 6 | 640 | 160 | 4 | 48 | 266 |
| 6 | 640 | 160 | 4 | 72 | 270 |
| 6 | 640 | 160 | 4 | ALL | 273 |
| 9 | 640 | 160 | 4 | 0 | 87 |
| 9 | 640 | 160 | 4 | 16 | 203 |
| 9 | 640 | 160 | 4 | 32 | 212 |
| 9 | 640 | 160 | 4 | 48 | 216 |
| 9 | 640 | 160 | 4 | 72 | 219 |
| 9 | 640 | 160 | 4 | ALL | 222 |
| 3 | 1280 | 320 | 4 | 0 | 156 |
| 3 | 1280 | 320 | 4 | 16 | 290 |
| 3 | 1280 | 320 | 4 | 32 | 297 |
| 3 | 1280 | 320 | 4 | 48 | 303 |
| 3 | 1280 | 320 | 4 | 72 | 309 |
| 3 | 1280 | 320 | 4 | ALL | 313 |
| 6 | 1280 | 320 | 4 | 0 | 57 |
| 6 | 1280 | 320 | 4 | 16 | 177 |
| 6 | 1280 | 320 | 4 | 32 | 183 |
| 6 | 1280 | 320 | 4 | 48 | 188 |
| 6 | 1280 | 320 | 4 | 72 | 192 |
| 6 | 1280 | 320 | 4 | ALL | 196 |
| 9 | 1280 | 320 | 4 | 0 | 37 |
| 9 | 1280 | 320 | 4 | 16 | 138 |
| 9 | 1280 | 320 | 4 | 32 | 143 |
| 9 | 1280 | 320 | 4 | 48 | 145 |
| 9 | 1280 | 320 | 4 | 72 | 147 |

**Table 5.4 Stress response of modeled whitetopping with distressed HMA. (cont.)**

| | | | | | |
|---|---|---|---|---|---|
| 9 | 1280 | 320 | 4 | ALL | 149 |
| 3 | 640 | 80 | 4 | 0 | 234 |
| 3 | 640 | 80 | 4 | 16 | 383 |
| 3 | 640 | 80 | 4 | 32 | 403 |
| 3 | 640 | 80 | 4 | 48 | 415 |
| 3 | 640 | 80 | 4 | 72 | 424 |
| 3 | 640 | 80 | 4 | ALL | 428 |
| 6 | 640 | 80 | 4 | 0 | 121 |
| 6 | 640 | 80 | 4 | 16 | 296 |
| 6 | 640 | 80 | 4 | 32 | 317 |
| 6 | 640 | 80 | 4 | 48 | 331 |
| 6 | 640 | 80 | 4 | 72 | 341 |
| 6 | 640 | 80 | 4 | ALL | 346 |
| 9 | 640 | 80 | 4 | 0 | 87 |
| 9 | 640 | 80 | 4 | 16 | 256 |
| 9 | 640 | 80 | 4 | 32 | 273 |
| 9 | 640 | 80 | 4 | 48 | 283 |
| 9 | 640 | 80 | 4 | 72 | 290 |
| 9 | 640 | 80 | 4 | ALL | 294 |
| 3 | 640 | 320 | 4 | 0 | 234 |
| 3 | 640 | 320 | 4 | 16 | 302 |
| 3 | 640 | 320 | 4 | 32 | 306 |
| 3 | 640 | 320 | 4 | 48 | 309 |
| 3 | 640 | 320 | 4 | 72 | 311 |
| 3 | 640 | 320 | 4 | ALL | 313 |
| 6 | 640 | 320 | 4 | 0 | 121 |
| 6 | 640 | 320 | 4 | 16 | 187 |
| 6 | 640 | 320 | 4 | 32 | 191 |
| 6 | 640 | 320 | 4 | 48 | 192 |
| 6 | 640 | 320 | 4 | 72 | 194 |
| 6 | 640 | 320 | 4 | ALL | 196 |
| 9 | 640 | 320 | 4 | 0 | 87 |
| 9 | 640 | 320 | 4 | 16 | 144 |
| 9 | 640 | 320 | 4 | 32 | 147 |
| 9 | 640 | 320 | 4 | 48 | 148 |
| 9 | 640 | 320 | 4 | 72 | 149 |
| 9 | 640 | 320 | 4 | ALL | 149 |

Figure 5.1 displays the critical stress development in a pavement with the following structural parameters:

- 4” PCC overlay
- 6” HMA layer
- Non-distressed HMA elastic modulus, 1280ksi
- Distressed HMA elastic modulus, 320ksi

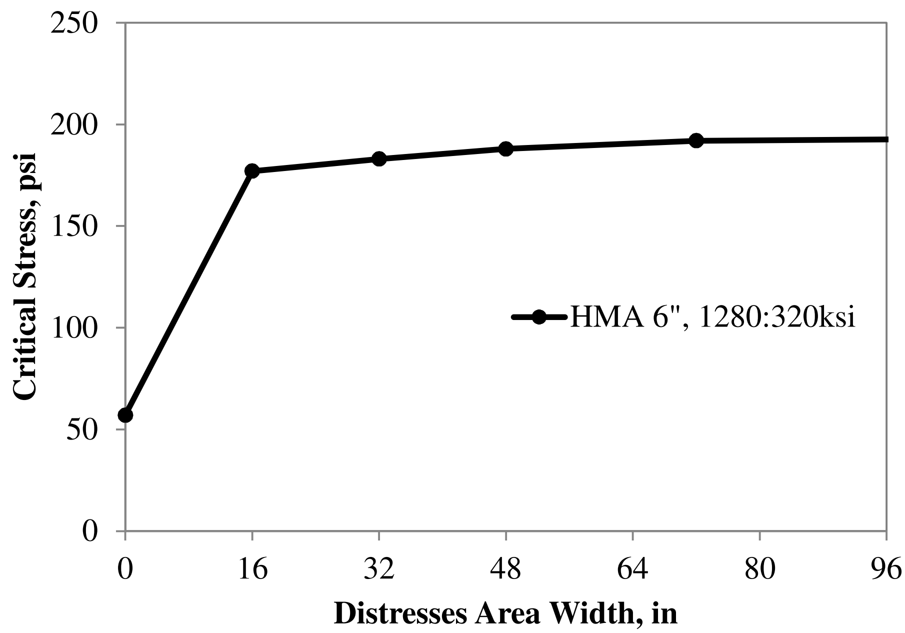


**Figure 5.1 Modeled critical stress development in whitetopping with structural properties specified above.**

As can be seen, the critical stress in the PCC layer increases significantly as the HMA distressed area approaches the smallest width investigated in this study, 16 inches. Assuming that the maximum critical stress (MCS) would occur when the entire HMA layer is at the reduced distressed stiffness, 90% of the MCS occurs at this initial distressed length. This result is representative of the other runs performed for this study where 86 to 97% of the MCS occurred at the smallest distress length of 16-in, as shown in Figure 5.2. As discussed previously, distressed areas with a smaller length than 16 inches create artificially high critical stresses, due to the increased influence of the abrupt transition at the boundary between non-distressed and distressed HMA. It was also felt that establishing an isolated area of reduced stiffness smaller than 16 inches would be unfeasible in the field, and thus would not be of practical significance.

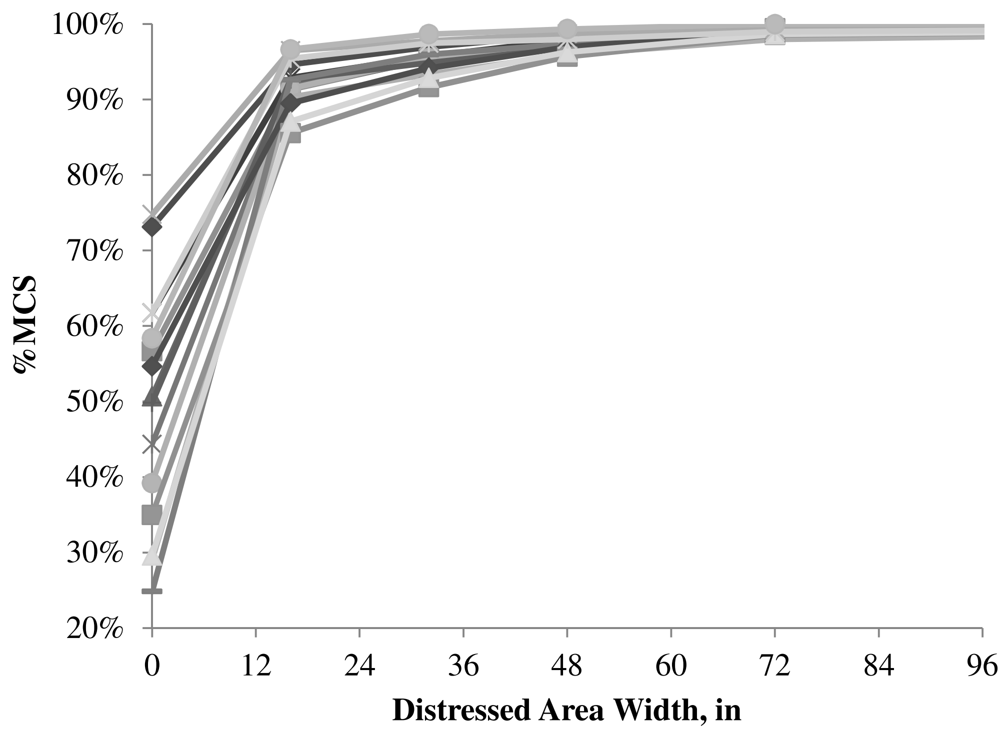


**Figure 5.2 Modeled critical stress development in whitetopping with distressed HMA.**

### 5.3 Effect of Modulus ratio on stress development

As described previously, the EMR between the non-distressed and distressed HMA is proposed to facilitate the approximation of stress development in the PCC overlay. To do this, the ratio of all damaged critical stress to all undamaged critical stress is shown to be a function of the modulus ratio (MR) which is the ratio of the damaged to that of the undamaged asphalt, Figure

5.3. The percentage of the MCS at a given distressed area size increases as the MR decreases. Equation 5.1 describes well, $R^2 = 0.97$, the results of runs with distressed areas 16" and greater.

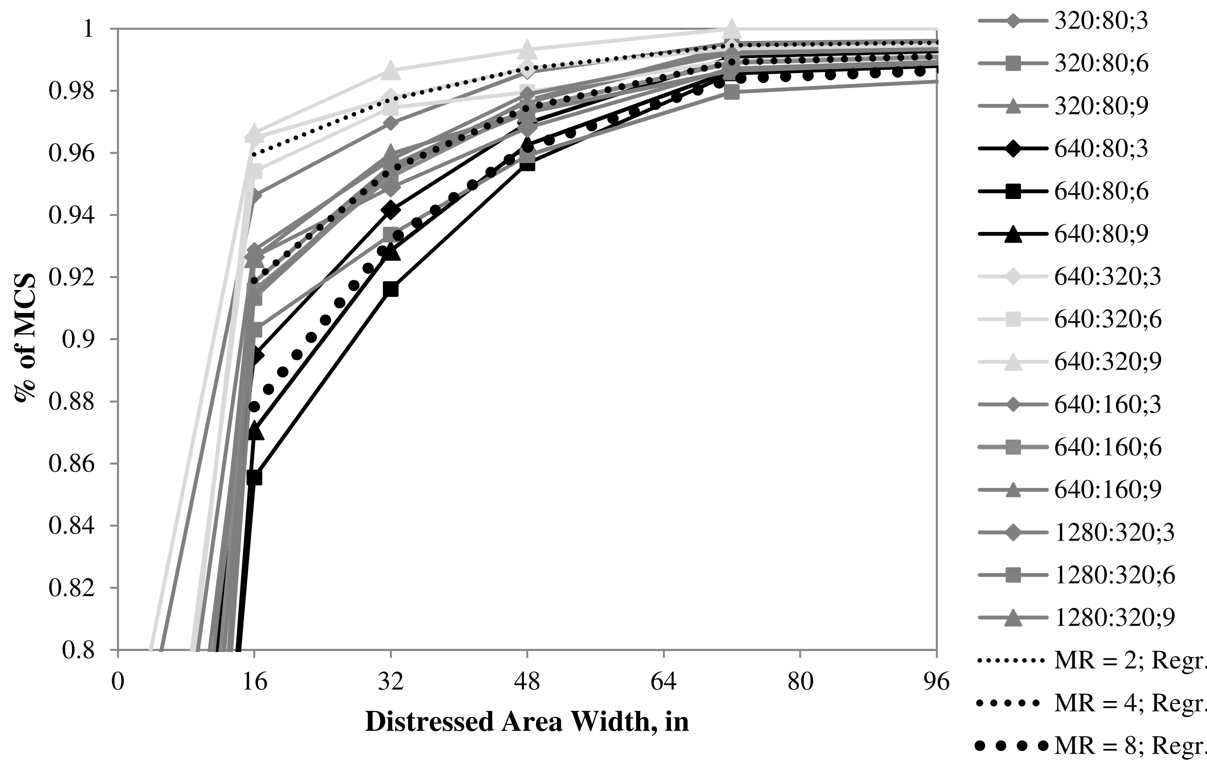


**Figure 5.3 Percentage of expected stress increase as a function of distressed area size with regression.**

$$\%MCS = 1 - 0.0585174 * ln(EMR) * exp[-0.0361307 * (x - 16)] \qquad Equation\ 5.1$$

*%MCS:* *percent of maximum critical stress*

*EMR:* *elastic modulus ratio, Es/Ew*

*x:* *distressed area width, in*

The proposed relationship between EMR and percent of MCS cannot be used for distress HMA sizes smaller than 16 inches. This is due to the increasing influence of the non-distressed HMA stiffness on the critical stress as the distressed area becomes less than 16 inches. For practical purposes, the exclusion of distressed area widths less than 16 inches is reasonable, as determining the stiffness for an area becomes more difficult as it becomes smaller.

When the non-distressed HMA stiffness is held constant, an increase in EMR for a constant size distressed area can inherently be expected to cause an increase in critical stress. As EMR increases, the stiffness of the distressed HMA decreases and this reduction in support detrimentally affects the performance of the thin bonded concrete overlay. Considering this expected behavior, the results from the modeling performed for this study are not surprising. The greater the EMR, the greater the critical stress increase.

Additional runs were performed to assess how well Equation 5.1 predicts %MCS for pavements with 3 inch PCC thickness. Table 5.5 presents the results from those runs, which show little difference between actual and predicted. This result verifies a key assumption discussed in Section 4.2.1, that the rate of stress increase due to increases in distressed area width is independent of PCC thickness for those thicknesses used in the design of ultra-thin and thin whitetopping pavements.

## 5.4 Implementing MCS Equation with Design Guide

The MCS prediction equation can be used for the design of thin whitetopping pavements by simply modifying the critical design stress based on an the estimated extent and severity of the distressed HMA. A procedure describing how the prediction equation can be used with the BCOA-ME design procedure is given as follows:

**Step 1. Evaluate the severity and extent of distress in existing HMA.**

Use any combination of the available pavement condition assessment methods to determine the following:

-Length of the shortest side of the distressed area

-Elastic modulus of undamaged HMA

-Elastic modulus of damaged HMA

Note that distressed area length of less than 16-inches cannot be used with the MCS prediction equation.

**Step 2. Determine %MCS**

Use the prediction equation to calculate %MCS using the information gathered in Step 1.

**Step 3. Calculate unmodified critical stresses**

Use the procedure prescribed in BCOA-ME to calculate the critical stress in the PCC layer separately using the undamaged and damaged HMA elastic modulus.

**Step 4. Modify the design critical stress based on %MCS**

The %MCS is multiplied by the difference between the critical stress calculated using the undamaged and damaged HMA elastic modulus. The product is then added to the undamaged critical stress to determine the design critical stress (modified to account for localized areas of distressed HMA). See Equations 5.2 and 5.3.

$$\sigma_{\text{undamaged}} - \sigma_{\text{damaged}} = \Delta_{\text{CS}} \qquad \textit{Equation 5.2}$$

$$\%\text{MCS} * (\Delta_{\text{CS}}) + \sigma_{\text{undamaged}} = \sigma_{\text{design}} \qquad \textit{Equation 5.3}$$

$\sigma_{undamaged}$: *critical stress calculated with undamaged HMA elastic modulus, psi*

$\sigma_{damaged}$: *critical stress calculated with damaged HMA elastic modulus, psi*

$\Delta_{CS}$: *change in critical stress between damaged and undamaged sections*

*%MCS: percent of maximum critical stress*

**Step 5. Continue BCOA-ME design procedure as normal**

**Table 5.5 Comparison of Actual and Predicted %MCS using Equation 5.1**

| $D_{HMA}$, in | $E_{HMA(undmg)}$, ksi | $E_{HMA(dmg)}$, ksi | $D_{PCC}$, in | Distressed Area Width, in | Actual %MCS | Predicted %MCS | Δ%MCS |
|---|---|---|---|---|---|---|---|
| 6 | 640 | 160 | 3 | 16 | 91% | 92% | -0.9% |
| 6 | 640 | 160 | 3 | 32 | 97% | 95% | 1.1% |
| 6 | 640 | 160 | 3 | 48 | 98% | 97% | 0.8% |
| 6 | 640 | 160 | 3 | 72 | 99% | 99% | 0.2% |
| 6 | 640 | 160 | 3 | all | 100% | 100% | 0.0% |
| 6 | 640 | 80 | 3 | 16 | 88% | 88% | 0.4% |
| 6 | 640 | 80 | 3 | 32 | 93% | 93% | 0.2% |
| 6 | 640 | 80 | 3 | 48 | 97% | 96% | 0.7% |
| 6 | 640 | 80 | 3 | 72 | 99% | 98% | 0.7% |
| 6 | 640 | 80 | 3 | all | 100% | 100% | 0.0% |
| 3 | 640 | 160 | 3 | 16 | 94% | 92% | 1.9% |
| 3 | 640 | 160 | 3 | 32 | 96% | 95% | 0.3% |
| 3 | 640 | 160 | 3 | 48 | 98% | 97% | 0.4% |
| 3 | 640 | 160 | 3 | 72 | 99% | 99% | 0.5% |
| 3 | 640 | 160 | 3 | all | 100% | 100% | 0.0% |
| 6 | 1280 | 160 | 3 | 16 | 88% | 88% | -0.3% |
| 6 | 1280 | 160 | 3 | 32 | 93% | 93% | -0.2% |
| 6 | 1280 | 160 | 3 | 48 | 97% | 96% | 0.3% |
| 6 | 1280 | 160 | 3 | 72 | 99% | 98% | 0.7% |
| 6 | 1280 | 160 | 3 | all | 100% | 100% | 0.0% |

The results from Table 5.2 verify another assumption, that the magnitude of stress increase is relatively constant for a given EMR regardless of the magnitude of difference between distressed and non-distressed HMA modulus. Figure 5.4 presents the results that demonstrate this behavior. At EMR equal to 4, a similar stress increase is found for a difference in modulus of 480-ksi as is for 960-ksi, when all other structural parameters are held constant.

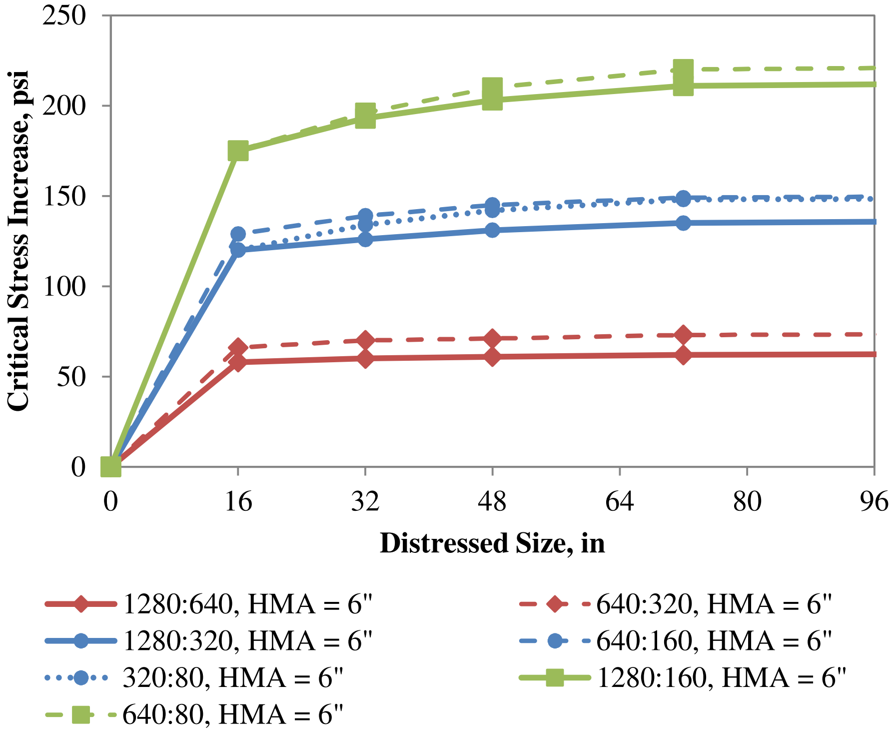


**Figure 5.4 Modeled stress increase at MR = 2, 4, and 8 with varying HMA stiffness.**

# 6 Conclusions

The results from this study of the effect of distressed HMA underlying thin bonded concrete overlays, indicate that even relatively small areas of diminished stiffness significantly increase critical stresses in the overlay. Distressed area sizes as small as 16-in caused an increase in stress that, for design purposes, are nearly the same as the entire HMA layer being at the reduced stiffness.

An approximation of the stress increase caused by an area of reduced stiffness in the HMA can be determined by first evaluating the level of stiffness reduction. Of the many proposed methods for evaluating in-situ pavements, correlation of deflection basin parameters (DBP) with layer elastic moduli is recommended. This is due to the ease in collecting the information necessary for such relationships, mainly FWD testing and limited coring to evaluate as-built layer thicknesses.

The size of the distressed HMA area is only useful if it can be determined for a distinct isolated area smaller than 48-in wide. Areas larger than this have critical stresses that are within 5% of the critical stresses for a pavement with the entire HMA layer at the reduced stiffness level.

Because of the difficulty in determining the exact boundary of areas with reduced HMA stiffness, it will often be the case that any pavement area evaluated as having a reduced stiffness will significantly increase the critical stress. To determine this reduction as accurately as possible, the effect of temperature on the backcalculated distressed moduli should be considered.

Based on the results of FWD testing at MnROAD, it was hypothesized that at elevated pavement temperatures the elastic modulus calculated for a distressed HMA layer decreased at a reduced rate as compared to a non-distressed HMA area. This is thought to be due to an improvement in the performance of cracks within the distressed area as the HMA softens. Further research is recommended to quantify the interaction between pavement temperature and the effect of distress on backcalculated HMA elastic moduli.

Preliminary FEM modeling indicated that the critical stress location changed depending on loading location. Since the likely loading location within the slab typically changes depending on the joint spacing, and different design procedures make different assumptions on where this critical stress occurs, the slab size should be considered when deciding which design procedure to use.

In addition to loading location, HMA stiffness also influenced the critical stress location in our FEM model. As the HMA stiffness increased, critical stresses moved from the bottom of the PCC layer to the top. It does not appear as though this change will significantly affect the design of thin whitetopping pavements, since at the stiffness at which the change occurs, minimum design layer thicknesses typically governs. Even so, research may be warranted considering this change in future design procedures.

## References

American Concrete Paving Association (ACPA). (1998). Whitetopping - State of the Practice. *Engineering Bulletin EB210P*.

ARA, Inc. ERES Consultants Division. (2004). *Guide for Mechanistic Empirical Design of New and Rehabilitated Pavement Structures.* Champaign, Illinois.

Chadbourn, B. (2003). *The use of FWD Deflections at the Mn/ROAD Test Facility to Determine Cracked HMA Modulus Values for Mechanistic Empirical Overlay Design.* Maplewood, MN: Minnesota Department of Transportation.

Crovetti, J. (1994). Evaluation of Jointed Concrete Pavement Systems Incorporating Open Graded Permeable Bases. *Ph.D. Dissertation, University of Illinois*. Urbana, Illinois.

Darter, M., Elliott, R., & Hall, K. (1991, September). Revision of AASHTO Pavement Overlay Design Procedure. *Transportation Research Board*. Washington, D.C.: National Cooperative Highway Research Program.

Darter, M., Hall, K., & Kuo, C.-M. (1995). *NCHRP Report 372: Support Under Portland Cement Concrete Pavements.* Washington, DC: Transportation Research Board, National Research Council.

Ioannides, A., & Korovesis, G. (1990). Aggregate Interlock: A Pure-Shear Load Transfer Mechanism". *Transportation Research Record 1286*.

Jung, Y. s., Zollinger, D. G., Won, M., & Wimsatt, A. J. (2009). *Subbase and Subgrade Performance Investigation for Concrete Pavement.* Springfield, VA: National Technical Information Service.

Kirchhoff, G. (1850). Uber das gleichfewichi und die bewegung einer elastishem scheibe. *J Fuer die Reine und Angewandte Mathematik, vol. 40*, 51-88.

Mack, J., & Chung Lung Wu, S. T. (1997). Model Development and Interim Design Procedure Guidelines for Ultra-thin Whitetopping Pavements. *Sixth International Purdue Conference on Concrete Pavement*, (pp. 231-256). West Lafayette, Indiana.

National Asphalt Pavement Association. (2009, March 31). Hearing on The Role of Research in Addressing Climate Change in Transportation Infrastructure Before the Subcommittee on Technology and Innovations.

National Concrete Pavement Technology Center. (2008). *Guide To Concrete Overlays, Second Edition.* Ames, Iowa: ACPA.

NCHRP. (2004). National Cooperative Highway Research Program Synthesis 338. Washington, DC: Transporation Research Board.

Portland Cement Association. (1984). Thickness Design for Concrete Highway and Street Pavements. *Publication No. EB109.01P*. Stokie, IL.

Rasmussen, R. O., McCullough, B. F., Ruiz, J. M., Mack, J., & Sherwood, J. A. (2002). Identificaiton of Pavement Failure Mechanisms at FHWA Aceelerated Loading Facility Ultrathin Whitetopping Project. *Journal of the Transportation Research Board 1916*, 148-155.

Riley, R., Titus-Glover, L., Mallela, J., Waalkes, S., & Darter, M. (2005). "Incorporation of Probablistic Concepts Into Fatigue Analysis of Ultrathin Whitetopping as Developed for the American Concrete Pavement Association. *Best Practices in Ultra Thin and Thin Whitetopping*, (pp. 288-317). Denver, Colorado.

Sheehan, M. J., Tarr, S. M., & Tayabji, S. (2004). *Instrumentation and Field Testing of Thin Whitetopping Pavement In Colorado and Revision of the Existing Colorado Thin Whitetopping Procedure.* Colorado Department of Transportation Research Branch.

Skarlatos, M. (1949). *Deflections and Stresses in Concrete Pavements of Airfields With Continuous Elastic Joints.* Mariemont, OH: U.S. Army Corps of Engineers.

Smith, G. (1993). W-h-i-t-e-t-o-p-p-i-n-g Spells Relief in Iowa. *Concrete Construction*, 792-798.

Thompson, M., III, A. B., & Baladi, G. (1989). ILLI-PAVE Based NDT Analysis Procedures. *ASTM STP 1026*, pp. 487-501.

U.S. Department of Transportation, R. a. (2011). *Transporation Statistics Annual Report 2010.* Washington, DC.

Vandenbossche, J. M. (2001, September). The Measured Response of Ultra-thin and Thin Whitetopping To Environmental Loads. Orlando, Florida: 7th International Conference on Concrete Pavements.

Vandenbossche, J. M. (2003). Performance Analysis of Ultrathin Whitetopping Intersections on US-169; Elk River, Minnesota. *Transportation Research Record*, 18-27.

Vandenbossche, J. M., & Barman, M. (2010). Bonded Whitetopping Overlay Design Considerations for Prevention of Reflection Cracking, Joint Sealing, and the Use of Dowel Bars. *Transportation Research Record 2155*, 3-11.

Vandenbossche, J. M., & Fagerness, A. J. (2002). Performance, Analysis, and Repair of Ultrathing and Thin Whitetopping at Minnesota Road Research Facility. *Transportation Research Record 1809*, 191-198.

Witczak, M., & Fonseca, O. (1996). Revised Predictive Model for Dynamic (Complex) Modulus of Asphalt Mixtures. *Transportation Research Record 1540*, 15-23.